7-2006

Coordination Environment: A New Approach to the Sensing of Lead (II) Itself

Kristina Marie Nespechal

COORDINATION ENVIRONMENT: A NEW APPROACH TO THE SENSING OF LEAD(II) ITSELF

by

Kristina Marie Nespechal

A Thesis
Submitted to the
Faculty of The Graduate College
in partial fulfillment of the
requirements for the
Degree of Master of Science
Department of Chemistry

Western Michigan University
Kalamazoo, Michigan
July 2006

ACKNOWLEDGMENTS

The entire journey is dedicated to my mentor, Dr. Marc W. Perkovic. I want to thank Dr. Perkovic for having faith in my abilities, and for guiding me through the research experience. Dr. Perkovic taught me to think beyond the scope of what had been previously researched by others, yet he taught me to learn from the previous literature. What a journey this thesis has been.

The journey began in Dr. Perkovic's Advanced Synthesis course. He drew five different macrocyclic structures on a page of paper and asked me to find out how to synthesize them. I ran off in a fever to the library, and I have never stopped the search for new ligand design. I found a unique world filled with geometrical design in his laboratory.

After searching for the perfect series to investigate, we began studying the photophysical behavior of lead(II) with the various macrocycles. Dr. Perkovic always had a vision, which was beyond most scientists I have encountered in my career. His patience, humor, and knowledge made him great.

Toward the end of the journey, I realized the gift that Dr. Perkovic had given me. Thank you for teaching me how to become a professional in the field. May other scientists venture onto your terrain in order to discover the rest of your story.

Kristina Marie Nespechal

COORDINATION ENVIRONMENT: A NEW APPROACH TO THE SENSING OF LEAD(II) ITSELF

Kristina Marie Nespechal, M.S.

Western Michigan University, 2006

Lead(II) is a silent poison that has plagued society since 3800 B. C. The average intake of lead in the United States alone is 50 μg per day, which is approximately 100-1000 times greater than that of prehistoric lead levels. Regardless of the banning of lead in paints and gasoline, lead poisoning prevails as a major environmental health risk. Science has the ability to address the concern with this environmental contaminant. The future production of an economical and reliable test kit for lead(II) relies on the luminescence of the heavy metal itself.

The absorption and emission spectra for a series of tetraaza lead(II) complexes (([12]aneN_4) lead(II) nitrate, ([14]aneN_4) lead(II) nitrate, ([15]aneN_4) lead(II) nitrate) were recorded in propylene carbonate at 298 K. In addition, molar absorbtivity, lifetime, and quantum efficiency data was collected.

Our investigation demonstrated that the ambient emissive properties of lead(II) itself are controlled via the distance this heavy atom resides above a tetraaza framework and by the stereochemical activity of the 'inert' lone pair of electrons on lead(II). The greater the distance lead(II) is from the tetraaza plane, the greater the emission intensity, lifetime, and quantum yield are.

TABLE OF CONTENTS

LIST OF TABLES

LIST OF FIGURES

List of Figures—continued

CHAPTER I

INTRODUCTION

Lead: An Analyte of Importance in Today's Society

Lead in the Environment

A child jumps off the school bus onto a main road of the town. The smiling child skips toward home while kicking up dust along the road. Happily, the child reaches a home, which was built in the 1940's. The home resides on a street that is known for antiquity, due to the stretch of homes along the street that were built during 1920-1950. A smiling parent greets their child at the front porch, and the parent hugs their dusty child. The child giggles in admiration toward the parent, while leaning against the paint of the original doorframe of the house. Together the parent and the child laugh; however, both are unaware of the silent poison that has been spread into their home and surrounds their everyday lives.

Lead is the silent poison that has plagued society since 3800 B. C. (1). In the United States alone, over 1.5 million children have elevated lead blood levels each year (2). The average intake of lead in the United States is 50 μg per day, which is approximately 100-1000 times greater than that of prehistoric lead levels (1,3). Regardless of the banning of lead in paints and gasoline, lead poisoning prevails as a major environmental health risk (1,2,3,4).

Reason for Concern

In today's world, lead is still used for a variety of purposes. As a result, ~300 million metric tons of lead enters the environment and resides in soil and dust (3).

Due to the accumulation of lead in soil and dust, lead can contaminate the food supply and pollutes rural and urban landscapes. Physical contact with 0.1 grams of dust may contain 10 μg or higher of lead (1). Due to the ease of entry into an individual, children are at extreme risk for lead poisoning.

Most cases of lead poisoning occur from exposure to divalent lead, Pb^{2+} (4). Divalent lead is the common form of lead in lead-based paint, which is a major cause of elevated lead blood levels in children (2,4). Many lead salts were used as pigments and as paint bases in homes and buildings built before 1980 (1,3). Children are exposed to these lead-ridden environments everyday. While the fractional absorption of lead in an adult is 7-15%, the fractional absorption of lead in children is 30-40% (1). The absorption rates in children are higher because children are more likely to play in the dirt and to place objects into their hands and mouths (2). Lead exposure causes impairments in a child's growth and interferes with the child's mental development (1,2). In addition, lead can inhibit the enzymes required for the biosynthesis of heme, causes the degeneration of nerve cells, is deposited into bones, and does not degrade once accumulated in the body (1,2). Lead does not discriminate; anyone can suffer the effects of lead accumulation in the body.

Science and the Concern

Due to the risk that the public faces in a lead-ridden environment, science has the capacity to address this concern. Typically the field of analytical chemistry can be used to detect concentrations of lead; however, the expense of portable equipment and equipment training places a financial burden on the average citizen and government agency. If a simple test kit could be created, then the public may have an economical method for testing for lead contamination. This test kit could be designed to be portable, inexpensive, and appropriate for field use by moderately trained individuals.

The science behind the test kit is the luminescence of the heavy metal itself; for example, lead(II) emits when coordinated to a non-emissive ligand. Lead(II) can be made to manifest its own luminescence when placed into an environment where its emissive behavior can be expressed. Through understanding its spectroscopic properties, the sensing of lead(II) itself can be made to be sensitive, selective, and have digital precision.

Lead(II): The Analyte of Focus

Few spectroscopic studies have been done on the coordination chemistry of lead(II) in solution (4). In addition, the sensing of lead(II) has relied on the notion that lead(II) is not emissive itself (5,6). The photophysical behavior of transition metals has been extensively investigated, yet a serious contaminant like lead has not been. Typically, sensor design utilizes a host-guest lead(II) system. The system's infrastructure consists of a molecular assembly tethered to a luminescent fragment, which is selective for a particular analyte such as lead(II) (7,8,9). The supramolecular host-guest lead(II) system does not rely on the emissive nature of lead(II) itself; the system depends on the association of lead(II) with the luminescent fragment (5,6,10,11). Upon association, the host-guest assembly's emissive properties are perturbed by allosteric manipulations (6,10), or by altering the system's electronic microenvironment (5,11).

Regardless of the disbelief in the luminescence of lead(II) itself, we contend that this heavy atom behaves as a sensor for itself. A recent study on the emissive behavior of a lead-bromide cluster implemented that at low temperatures an intralead transition occurred (12). Therefore, the host-guest system is not necessary for the detection of lead(II). Vogler's study on the luminescence of lead(II) chloride complexes in solution determined that $PbCl_3^-$ and $PbCl_4^{2-}$ species were highly

emissive in solution at room temperature (13). Thus, previous investigations on the luminescence of lead(II) in solution have shown that lead is emissive itself.

We propose that if the analyte in question can absorb energy, the analyte should emit this energy via a radiative decay process.

The selection rules for absorption and emission are based on the same set of rules (14,15,16):

1. Spin Selection Rule: A radiative transition must have no change in the total spin quantum number, S. Thus, a transition between a singlet state ($\Delta S = 0$) and a triplet state ($\Delta S = 1$) is spin forbidden. However, a heavy atom such as lead(II) allows a forbidden transition to occur through spin-orbit coupling.

2. Orbital Symmetry Selection Rule: The orbital angular momentum, l, must be conserved when a photon is emitted or absorbed, $\Delta l = +/- 1$. A transition involving a large change in the orbital angular momentum is forbidden unless vibronic coupling exists.

3. The Laporte Selection Rule: The only allowed transitions are those accompanied by a change in parity. A forbidden transition that involves no change in parity is allowed when the removal of the centre of symmetry creates a vibronically allowed transition. A d-d transition is often forbidden but seen due to an asymmetric vibration.

4. The Franck-Condon Principle: Radiative transitions occur more rapidly than nuclear motions; therefore, the geometry of the molecule is conserved. However, this rule does not need to be obeyed for radiative relaxation.

Vogler's luminescence study on lead(II) chlorides implemented that lead(II) can be considered in terms of the metal centered *s-p* transitions of the free s^2 ion (13,17). The radiative relaxation route back down to the ground state is shown in Figure 1 (13,17). We suggest that the transitions may be considered as *d-d* transitions

of the d^2 ion under the influence of an octahedral field, which is illustrated in Figure 2 (15,16).

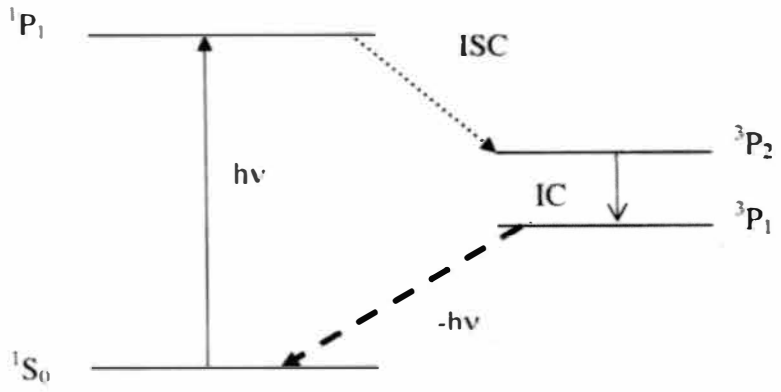

hν = absorption, IC = internal conversion, ISC = intersystem crossing, -hν = phosphorescence, $^1S_0$ = term symbol for the singlet ground state, $^1P_1$, $^3P_2$, $^3P_1$ = term symbols for the singlet and triplet excited states, respectively

Figure 1. Jablonski Diagram for the Metal Centered *s-p* Transitions of the s^2 Ion (Vogler; et. al.).

Source: Vogler, A.; Nikol, H. The Structures of s^2 Metal Complexes in the Ground and sp Excited States. *Comments Inorg. Chem.* **1993,** *14*, 245-261., Nikol, H.; Becht, A.; Vogler, A. Photoluminescence of Germanium(II), Tin(II), and Lead(II) Chloride Complexes in Solution. *Inorg. Chem.* **1992,** *31*, 3277-3279., Claudio, E. S.; Godwin, H. A.; Magyar, J. S. Fundamental Coordination Chemistry, Environmental Chemistry, and Biochemistry of Lead(II). In *Progress in Inorganic Chemistry*, Vol. 51; Karlin, K. D., Ed.; John Wiley & Sons, Inc.: NY, 2003; pp 1-144.

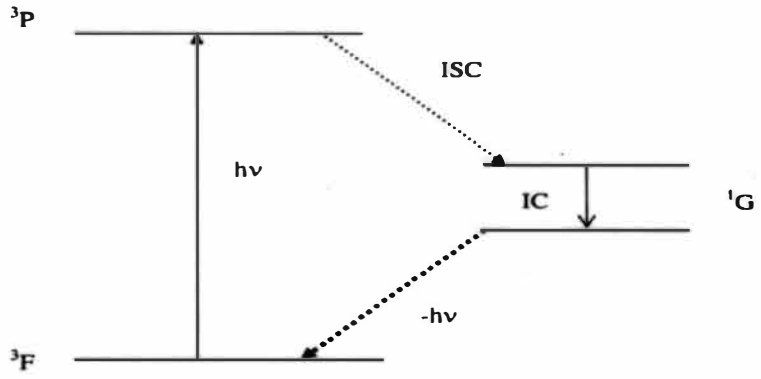

hν = absorption, IC = internal conversion, ISC = intersystem crossing, -hν = phosphorescence, ^3F = term symbol for the triplet ground state, ^3P, ^1G = term symbols for the triplet and singlet excited states, respectively

Figure 2. Jablonski Diagram for the *d-d* Transitions of the d^2 Ion under the Influence of an Octahedral Field (Lever; et. al.).

Source: Lever, A. B. P. *Inorganic Electronic Spectroscopy*; Elsevier Publishing Company: NY, 1968; pp 1-18, 123-150., Kettle S. F. A. *Physical Inorganic Chemistry: A Coordination Chemistry Approach*; Oxford University Press: NY, 1998; pp 156-182, 455-458.

Regardless of the choice of electronic environment for lead(II), the selection rules listed above are followed or are relaxed, forbidden transitions become weakly allowed. If lead(II) absorbs a photon based on the selection rules, then it emits the photon based on the same selection rules as long as thermal relaxation is controlled. As a result, the heavy atom emits. In terms of either the s^2 or d^2 electronic environment, the following occurs in contention with the selection rules listed above:

1. The metal centered *s-p* absorption maximum corresponds to excitation from a singlet ground state to that of a singlet excited state, which is accompanied with a relatively large molar extinction coefficient (13). With regard to the possible *d-d* transitions, the absorption maximum corresponds to excitation from a triplet ground state to that of a triplet excited state.

2. Absorption of a photon results in lead(II) discarding its excitation energy via radiative decay in the ultra violet or visible region of the electromagnetic spectrum. Due to spin-orbit coupling, intersystem crossing is facilitated and radiative relaxation is from an excited triplet state back down to the singlet ground state (13,17) or vice versa for the *d-d* transitions.

3. The Laporte Selection Rule is abided by for each transition, absorption or emission, in terms of the *s-p* transitions (17). However, if lead(II) manifests its electronic behavior as that of the possible *d-d* transitions, this selection rule becomes relaxed through vibronic coupling and spin-orbit coupling.

While the selection rules support that lead(II) can absorb and emit light, the ability to design a sensor to express this photophysical behavior of lead(II) becomes important. Therefore, we intend on defining specific parameters required for the sensing of lead(II) itself.

Previous investigations have shown that the size of the macrocyclic ring and the replacement of oxygen donor atoms with nitrogen donor atoms in the macrocyclic framework are related to complex stability and selectivity (18,19).

Hancock's team discovered that the selectivity of tetra-(2-hydroxypropyl)-[12]aneN_4 for a large lead(II) ion over a small zinc(II) ion was lower than anticipated when compared to that of tetra-(2-hydroxyethyl)-[14]aneN_4 (18). As a result of Hancock's discovery, the stereochemical activity of the 'inert lone pair', the $6s^2$ electron pair of lead(II), became pertinent to the Pb/Zn selectivity data. The 'inert

lone pair' affects the geometry of a lead(II) coordination complex. For example, an active $6s^2$ electron pair requires the ligands to be hemidirected; there is a vacant site in the coordination sphere with the ligand clustered on one side of the lead(II) ion (3,20). If the lone pair of electrons is stereochemically inactive, the complex is holodirected with the ligands evenly distributed about the lead(II) ion (3,20). The schematics for hemidirected, 'active', and holodirected, 'inactive', lead(II) complexes are depicted in Figure 3.

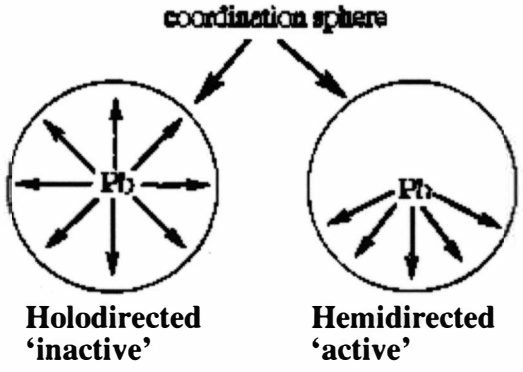

Figure 3. Hemidirected and Holodirected Coordination of Lead(II) (Shimoni-Livny; et. al.).

Source: Shimoni-Livny, L.; Glusker, J. P.; Bock, C. W. Lone Pair Functionality in Divalent Lead Compounds. *Inorg. Chem.* **1998,** *37*, 1853-1867.

In hemidirected lead(II) complexes, there is *s* and *p* character in the lone pair orbital; however, the holodirected lead(II) complexes have the lone pair residing in a spherically symmetrical *6s* orbital (3,18). 'Active' lead(II) complexes have lead(II) behaving as a small ion, such as zinc(II), and result in a Pb-N bond length range of 2.37 Å to 2.56 Å (18). In comparison, an 'inactive' lead(II) complex displays a departure from the covalency observed with 'active' complexes because the Pb-N

bond length range increases to 2.62 Å to 2.88 Å (18).

Apart from stereochemical activity, it has been shown that the formation constants of lead(II) complexes of various tetraaza macrocycles differ significantly as the size of the macrocycle is increased. Hancock's team found that there is a preference of binding for lead(II) with [12]aneN$_4$ over that of [13]aneN$_4$ and [14]aneN$_4$ (19). In addition, Hancock's team indicated that the most favorable conformers for [12]aneN$_4$ and [14]aneN$_4$ lead(II) complexes were the trans-I conformer of [12]aneN$_4$ and the cis-V or trans-I conformer of [14]aneN$_4$ shown in Figure 4 (19).

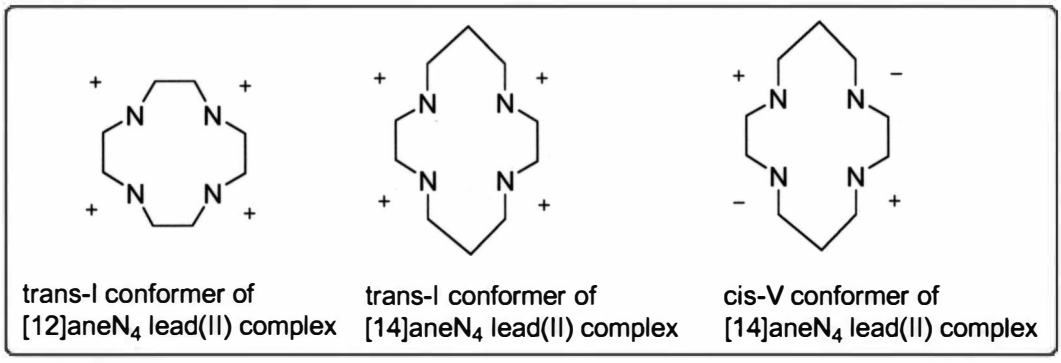

The cis or trans prefix indicates the position of the counterion, such as nitrate in our complexes. The +/- signs indicate whether the hydrogens on the nitrogens lie above or below the plane of the page.

Figure 4. Conformers of [12]aneN$_4$ and [14]aneN$_4$ lead(II) Complexes (Thom; et. al.).

Source: Thom, V. J.; Hosken, G. D.; Hancock, R. D. Anomalous Metal Ion Size Selectivity of Tetraaza Macrocycles. *Inorg. Chem.* **1985,** *24*, 3378-3381.

Thus, the long Pb-N bond lengths found for each macrocycle (2.5 Å to 2.7 Å) are tolerant of considerable Pb-N bond distortions (19). The Pb-N bond distortions

place lead(II) out of the plane of the four nitrogen donor atoms in the macrocycle (19); such that, the distance lead(II) lies above the plane should differ for tetraaza macrocycles of varying size.

Hancock's lead(II) activity experiments and molecular mechanics calculations on tetraaza macrocycles led us to conceive that the emissive nature of lead(II) itself could be related to the stereochemical activity of lead(II). Belmer of Kalamazoo College investigated the relationship between the stereochemical activity of lead(II) and the emissive behavior of lead(II), during the Summer 2005 Research Experiences for Undergraduates (REU) program at Western Michigan University (21). Belmer investigated two tetraaza complexes, ([12]aneN$_4$) lead(II) nitrate and (tetra-(2-hydroxypropyl)-[12]aneN$_4$) lead(II) nitrate (21). ([12]aneN$_4$) lead(II) nitrate is a sterochemical 'active' complex, while (tetra-(2-hydroxypropyl)-[12]aneN$_4$) lead(II) nitrate is a stereochemical 'inactive' complex (18). Belmer found that there were distinct differences in the optical properties of each complex (21). For example, the emission of (tetra-(2-hydroxypropyl)-[12]aneN$_4$) lead(II) nitrate in propylene carbonate was extinct at 180 K with a delay time of 2 μs and a gate width of 5 μs (21). ([12]aneN$_4$) lead(II) nitrate in propylene carbonate became highly emissive under the same conditions as shown in Figure 5 (21).

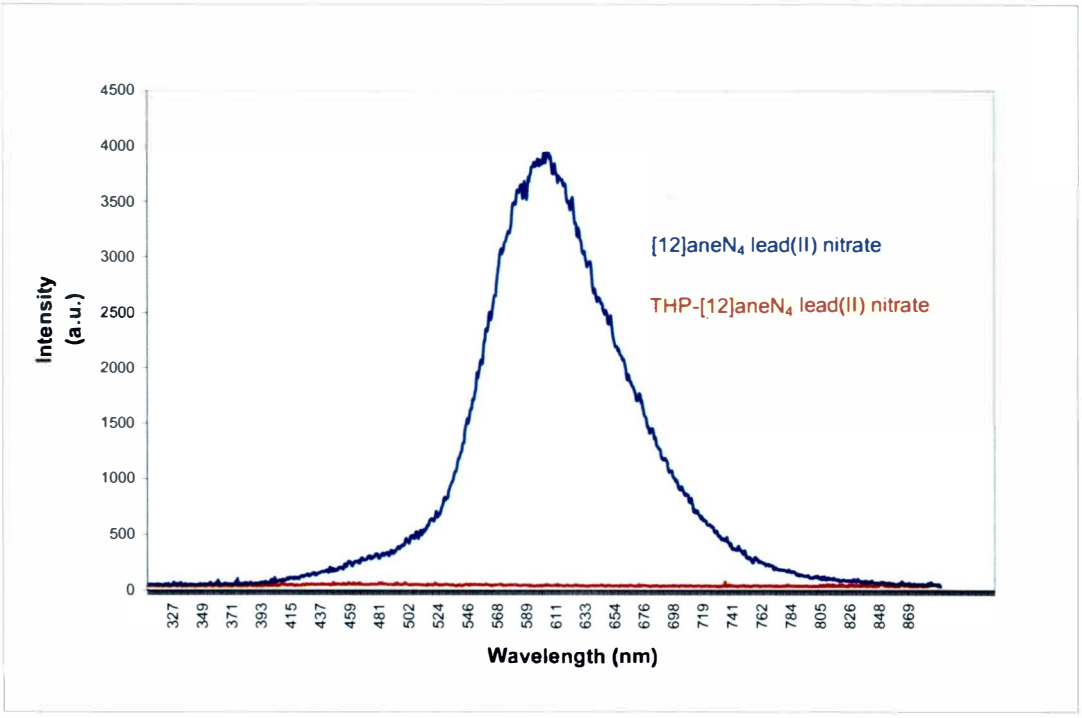

266 nm excitation, 2μs delay, 5 μs gate width

Figure 5. Luminescence Spectra of ([12]aneN$_4$) lead(II) nitrate and (tetra-(2-hydroxypropyl)-[12]aneN$_4$) lead(II) nitrate in Propylene Carbonate at 180 K (Belmer; Perkovic).

Source: Belmer, N. (2005). Western Michigan University Summer REU Program. Used with permission of Dr. Marc. W. Perkovic, REU research advisor, Chemistry Department, Western Michigan University, 3-13-06.

The preliminary observations from Belmer's research (21) supported our postulate: the luminescence of lead(II) is related to the stereochemical activity of the 6s^2 lone pair of lead(II). The 'activity/inactivity' of the lone pair of lead(II) exhibits a binary emission response, on-off. In addition to Belmer's study, we became interested in the emission response of lead(II) toward changes in the macrocyclic framework. The changes in the framework are a result of changing the size of the tetraaza

macrocyclic cavity, which alters the distance lead(II) rests above the plane of the macrocycle. The distance that lead(II) rests above the tetraaza plane is a parameter, which we can control the photophysical behavior of lead(II) with. The control of the emissive behavior of lead(II) allows for determination of the variables necessary for proper sensor (test kit) development. Our investigation focuses on a series of lead(II) complexes, which involves the coordination of lead(II) nitrate to a tetraaza macrocyclic framework. The series of macrocyclic complexes investigated are: ([12]aneN$_4$) lead(II) nitrate, ([14]aneN$_4$) lead(II) nitrate, and ([15]aneN$_4$) lead(II) nitrate (Figure 6).

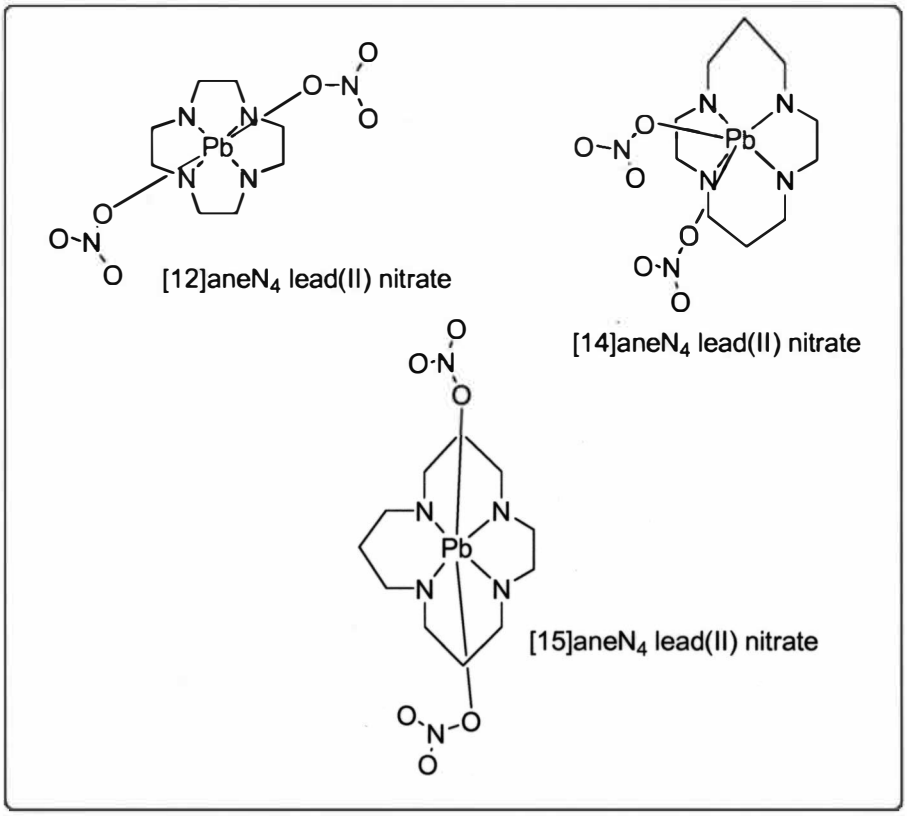

The hydrogens on the nitrogens are not shown.

Figure 6. Lead(II) nitrate Tetraaza Complexes Investigated.

Through geometrical manipulation of the Pb-tetraaza plane distance using the series shown above, we will probe the emissive nature of lead(II). Thus, we propose that the emissive behavior of lead(II) itself depends on the stereochemical activity of the 'inert' lone pair of electrons and on the size of the macrocyclic framework of the complex. We expect to observe the luminescence of lead(II) when the $6s^2$ lone pair is active; however, we also expect to observe changes in the optical response of lead(II) based on the differences in the distance lead(II) lies above the plane of the macrocycle.

CHAPTER II

RESULTS ON THE INDIVIDUAL COMPLEXES

Analysis on the Lead(II) Complexes

([12]aneN$_4$) lead(II) nitrate

In order to verify successful complexation of $Pb(NO_3)_2$ with [12]aneN$_4$, the presence of N-H stretching, C-H stretching, and the N-O stretch from the nitrate counterions were verified by IR spectroscopy (Figure 9). In addition, the IR spectrum of the complex was compared to that of $Pb(NO_3)_2$ and the free ligand and (Figure 7 and Figure 8).

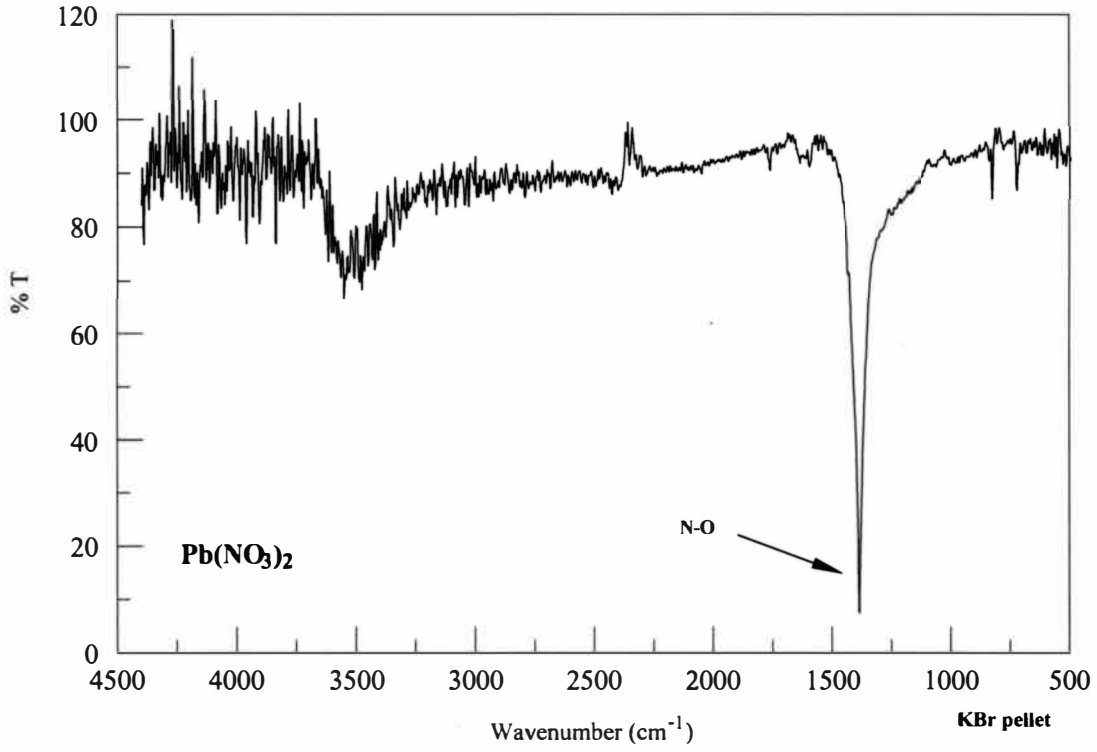

Figure 7. The IR Spectrum of Lead(II) nitrate.

The N-O stretch for lead(II) nitrate is present at ~1375 cm^{-1}. After complexation with [12]aneN_4, the N-O stretch will be shifted.

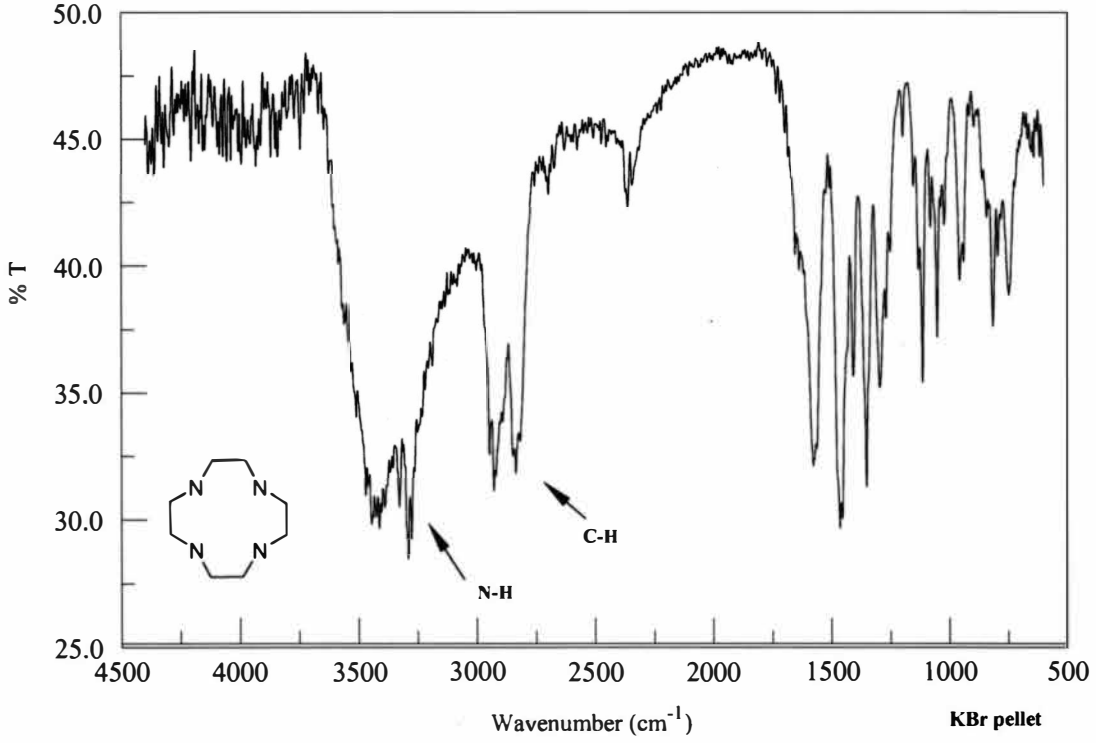

Hydrogens on the nitrogens are not shown.

Figure 8. The IR Spectrum of the Free Ligand, [12]aneN_4.

N-H stretching for the free ligand was observed at ~3291 cm^{-1}, and the asymmetric and symmetric saturated C-H stretches were found below 3000 cm^{-1} (2928 cm^{-1} and 2835 cm^{-1}). These stretches will be shifted like the N-O stretch for $Pb(NO_3)_2$, upon successful complexation.

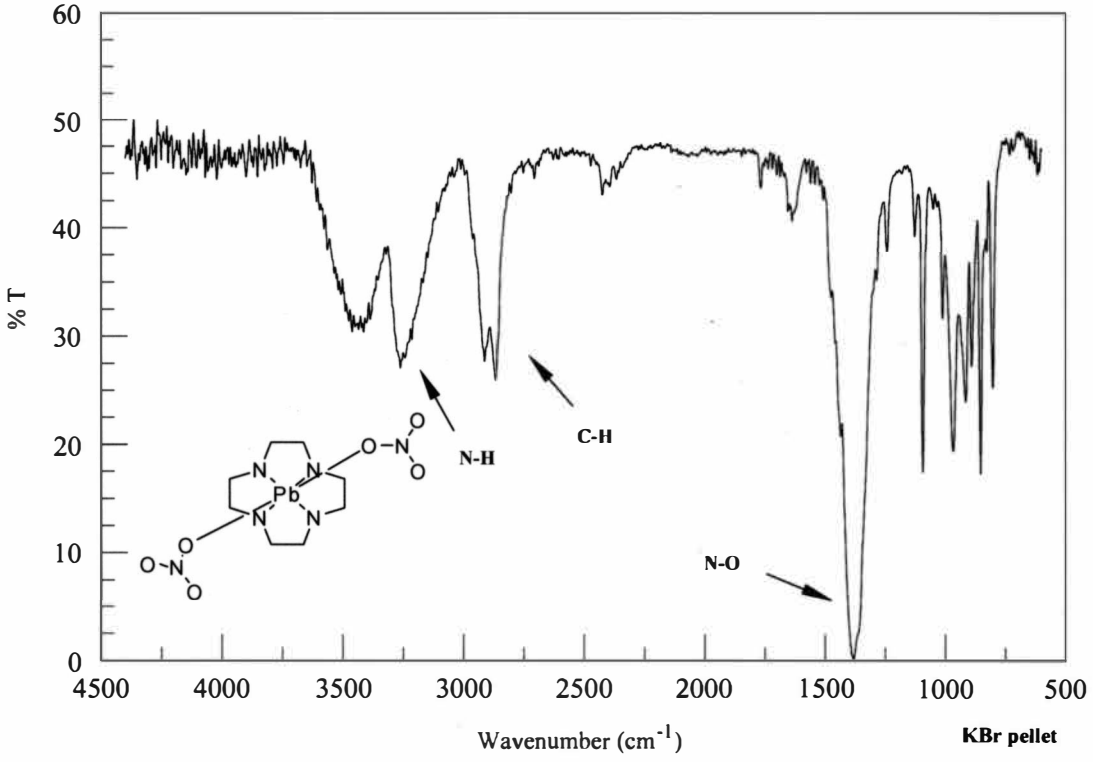

Hydrogens on the nitrogens are not shown.

Figure 9. The IR Spectrum of ([12]aneN$_4$) lead(II) nitrate.

The N-H, C-H, and N-O stretches (3263 cm^{-1}, 2990 and 2867 cm^{-1}, 1381 cm^{-1} respectively) were observed for the complex; also, each stretch was at a different wavenumber than the observed stretches shown for $Pb(NO_3)_2$ and the free ligand in Figure 7 and Figure 8. As a result of the significant shifts in stretching frequencies, complexation of the free ligand with $Pb(NO_3)_2$ was verified.

The ^{13}C NMR for the complex was recorded at room temperature in DMSO-d_6 and the following was obtained: 1C at δ(ppm) 45.80. The ^{13}C spectrum is shown in Figure 10. The ^{13}C NMR spectrum for the free ligand in DMSO-d_6 has 1C at δ(ppm) 45.76. The absence of a significant shift in resonance for the complex's ^{13}C signal may be due to preservation of symmetry upon complexation of the free ligand with

$Pb(NO_3)_2$. Regardless of the presence of the heavy metal, each carbon in the macrocycle remains in a similar environment to that of the free ligand.

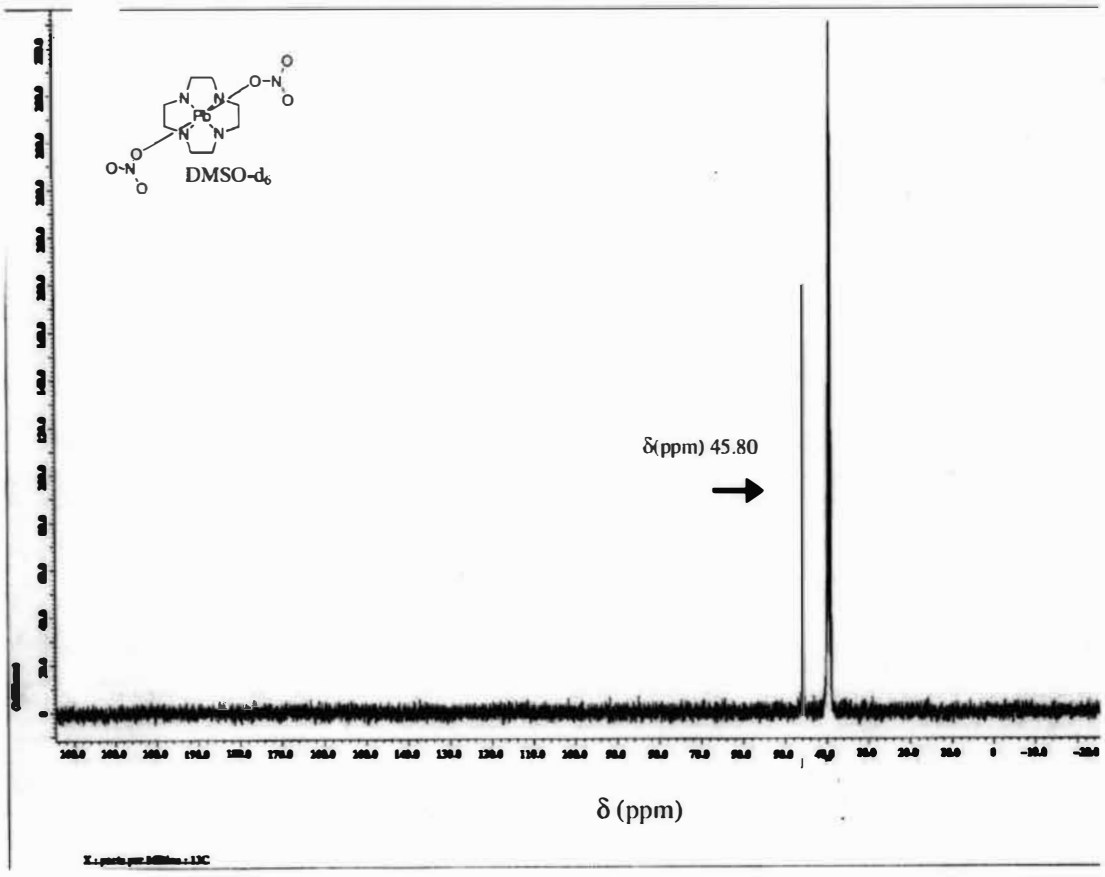

Figure 10. ^{13}C NMR Spectrum of ([12]aneN$_4$) lead(II) nitrate in DMSO-d_6 at 298 K.

X-ray quality crystals of ([12]aneN$_4$) lead(II) nitrate were unable to be produced, due to decomposition upon exposure to the atmosphere. However, the complex of ([12]aneN$_4$) lead(II) perchlorate was prepared and analyzed. The perchlorate of the complex provided a more stable sample for x-ray analysis. In order

to maintain that the geometry of both complexes were comparable, the absorption band at 249 nm and yellow-green emission band at 540 nm for ([12]aneN$_4$) lead(II) perchlorate were obtained and verified with the experimental results for ([12]aneN$_4$) lead(II) nitrate. The x-ray quality crystals produced were of the monoclinic system and P2$_1$/n space group, a non-standard setting of the P2$_1$/c, No. 14. The complex was weakly coordinated to DMSO, which can be seen in Figure 11 (22).

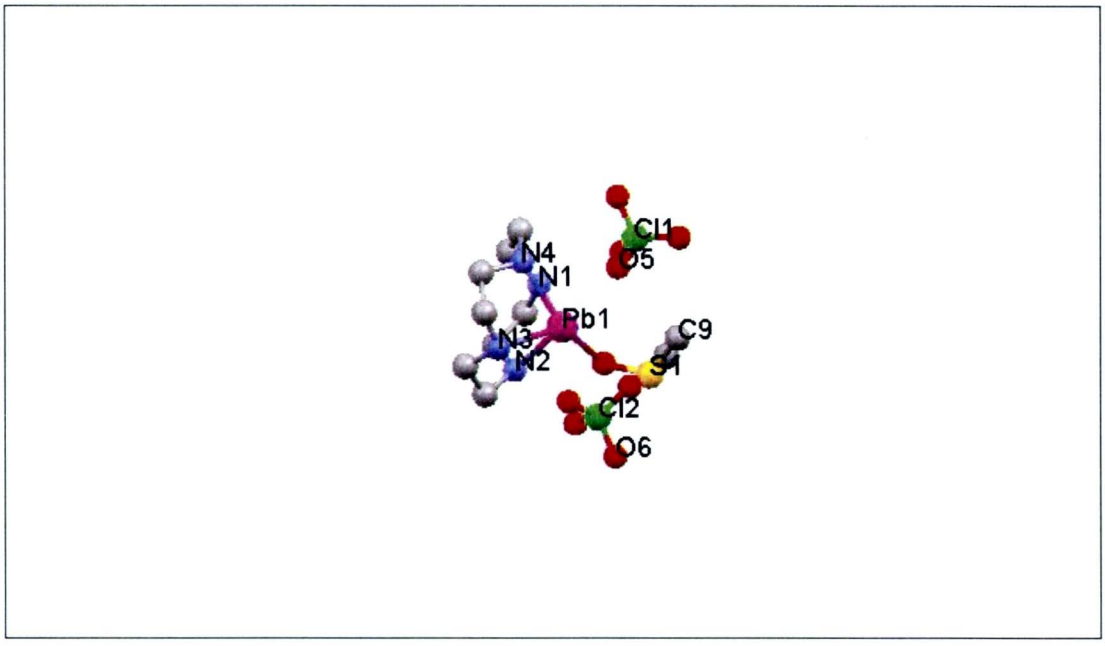

The color scheme is: C (gray), N (blue), O (red), Cl (green), S (yellow), Pb (pink). Atoms of interest are the labeled nitrogens.

Figure 11. Structure of ([12]aneN$_4$) lead(II) perchlorate (Heeg).

Source: Heeg, M. J. (2006). Wayne State University. The .cif file was used with permission of Dr. Mary Jane Heeg, X-ray Laboratory Manager, Chemistry Department, Wayne State University, 3-31-06.

A list of Pb-N bond length and angle data is located in Table 1 (22). The data in Table 1 (22) was used to obtain the distance that lead(II) rests above the plane of

the macrocycle.

Table 1: Selected Bond Lengths (Å) and Angles (degrees).

	Bond Lengths		
Pb(1) – N(1)	2.480	Pb(1) – N(3)	2.560
Pb(1) – N(2)	2.482	Pb(1) – N(4)	2.569
	Bond Angles		
Pb(1) – N(1) – N(2)	54.26	Pb(1) – N(3) – N(2)	54.04
Pb(1) – N(1) – N(4)	56.39	Pb(1) – N(3) – N(4)	55.47
Pb(1) – N(2) – N(1)	54.22	Pb(1) – N(4) – N(1)	53.52
Pb(1) – N(2) – N(3)	56.63	Pb(1) – N(4) – N(3)	55.19

Using computational software with the experimental data from Table 1, the calculated distance for lead(II) above the plane of [12]aneN$_4$ is 1.472 Å. Due to this distance, we expect to see an absorption band characteristic of lead(II) within this spatial environment.

The absorption spectrum for ([12]aneN$_4$) lead(II) nitrate was compared to that of the free ligand, Pb(NO$_3$)$_2$, and the solvent (Figure 12). The acquisition of a unique absorption spectrum was proof that the complex was its own species in solution. We found that the complex had a relatively long shelf life in solution because decomposition products or changes in the absorption features were not found after several weeks.

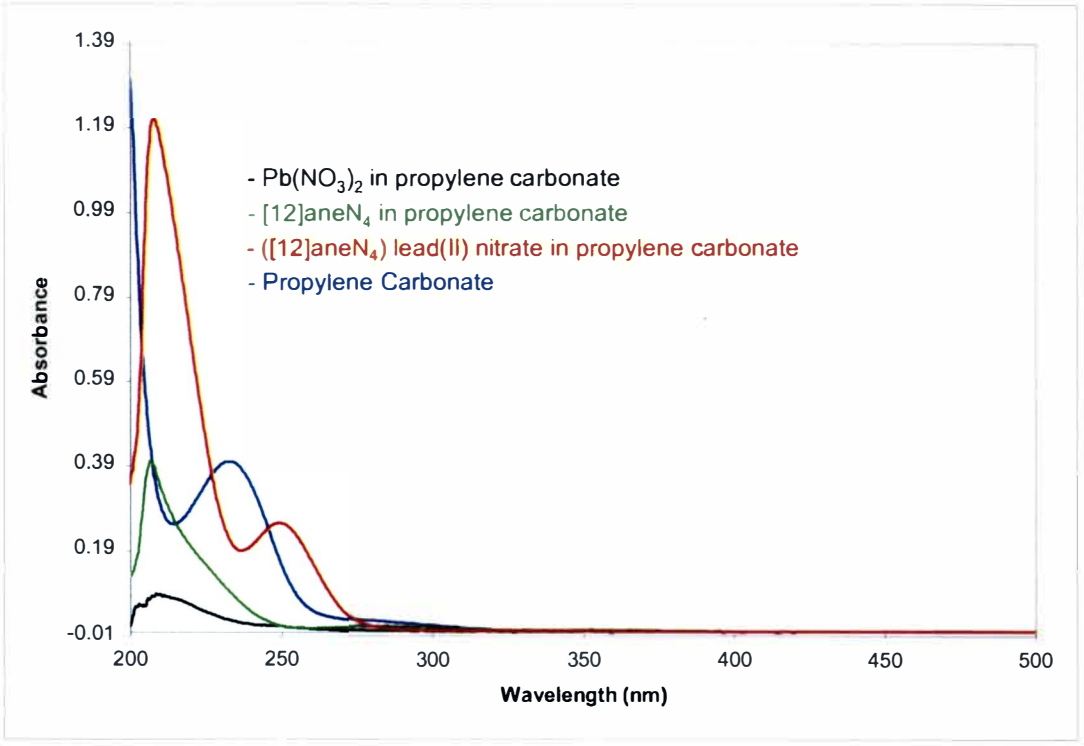

All solids were dissolved in propylene carbonate. All the UV-vis spectra for the solid samples dissolved in propylene carbonate were solvent subtracted.

Figure 12. UV-vis Spectra of ([12]aneN$_4$) lead(II) nitrate, [12]aneN$_4$, Pb(NO$_3$)$_2$, and Propylene Carbonate at 298 K.

The complex shown in Figure 12 absorbed radiation in the ultraviolet region of the electromagnetic spectrum and had a maximum wavelength of 249 nm. The complex had a molar absorbtivity (ε) of 3080 L mol^{-1} cm^{-1}, which indicated that a spin allowed transition occurred upon absorption of radiation. Excitation at 266 nm was possible, due to the 249 nm absorption band. The emission spectrum of the complex in solution was unique as well; such that, the spectral features obtained were not the same as the free ligand or the solvent features shown in Figure 13.

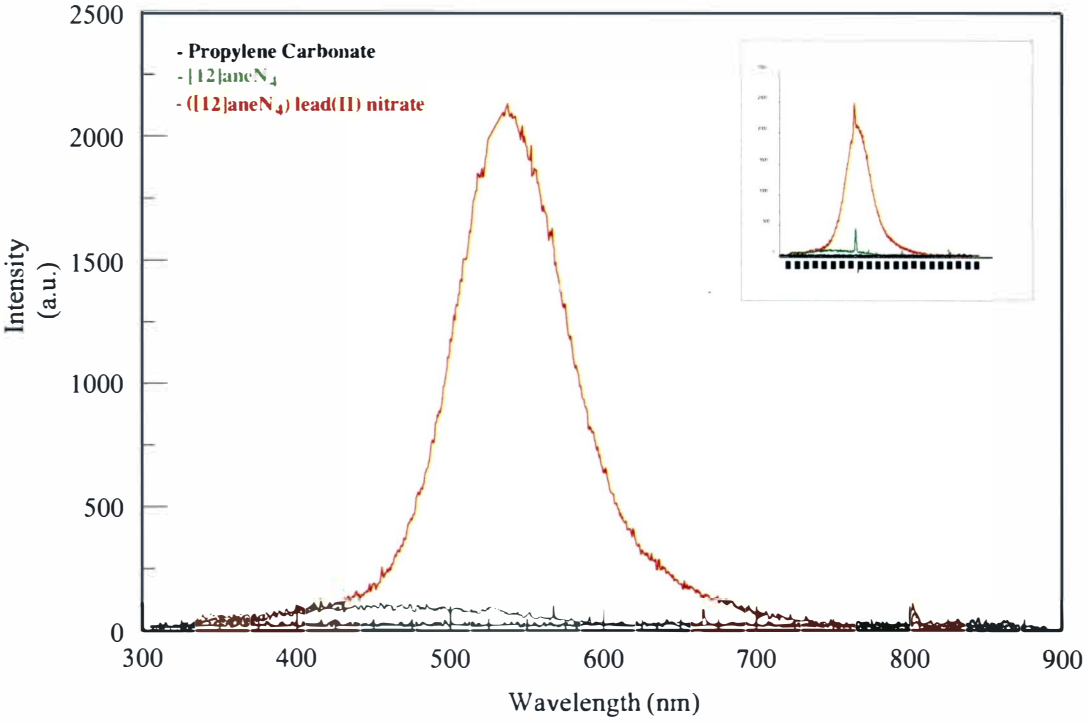

The complex is shown in red and is compared to the spectra for the free ligand (green) and the solvent (black). All samples were deaerated with He to avoid quenching by O_2; in addition, all variables for acquisition of the emitted light were kept the same (266 nm excitation; 180 ns delay; 5 μs gate width; 25 second exposure). A spike from charge build-up on the CCD was taken out of each spectrum and the data points were interpolated from 525.97 nm to 534.56 nm (inset shows spike). A laser spike is present near 800 nm.

Figure 13. Luminescence Spectrum of ([12]aneN$_4$) lead(II) nitrate in Propylene Carbonate at 298 K.

As seen in Figure 13, the emission response was not due to the presence of the ligand in solution or the solvent. Therefore, the emission was due to a highly luminescent lead(II) center. The maximum wavelength of the emission band was at 540 nm and the lifetime, τ, of the luminescent center was 5.47 +/- 0.36 μs. Due to the relatively long lifetime, the emissive behavior of the complexed lead(II) center was caused by relaxation through phosphorescence from a spin forbidden state. Typically, phosphorescent lifetimes are on the order of microseconds to several seconds (23).

Shorter lifetimes are indicative of fluorescence, which are on the order of 10^{-8} seconds (23). In addition to the radiative relaxation seen for the emissive lead(II) center, this emissive behavior was found to be quenched by the presence of O_2. The quenching of the emission response is shown in Figure 14.

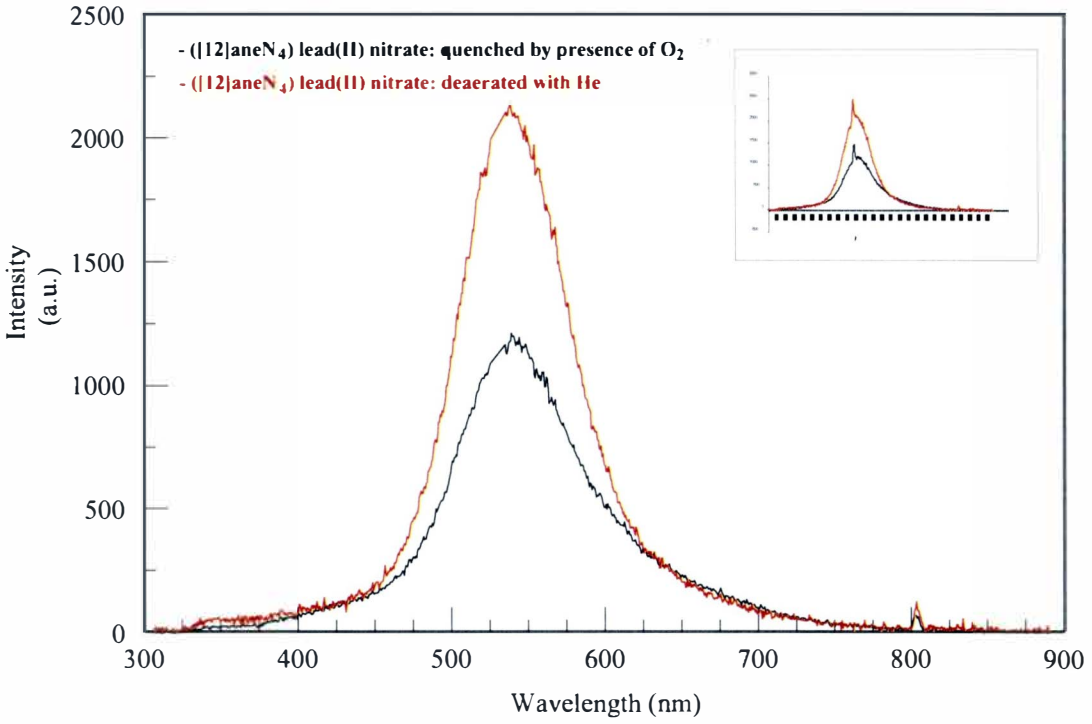

The deaerated sample is shown in red, and the aerated sample is shown in black. Both samples were recorded at 298K with a 266 nm excitation, 180 ns delay, 5μs gate width, and a 25 second exposure time. A spike from charge build-up on the CCD was taken out of each spectrum and the data points were interpolated from 525.97 nm to 534.56 nm (inset shows spike).

Figure 14. The Quenching of ([12]aneN$_4$) lead(II) nitrate by the Presence of O_2 in Propylene Carbonate at 298 K.

In addition to quenching by O_2, the emissive behavior of ([12]aneN$_4$) lead(II) nitrate was temperature dependent. Since kT from the Boltzmann Distribution is relatively small at room temperature, the energy gap between the two states (either Figure 1 or Figure 2) is small. Also, internal conversion from the upper excited state

down to the lower excited state is a fast process (23). It's possible that the emission band seen at 298 K is a combination of relaxation from the two spin-forbidden excited states. At low temperatures it's possible that the energy gap between the two excited states becomes quite large and competition between the two populated states exists. This competition at 180 K is illustrated in Figure 15. After cooling, the sample was warmed to room temperature to ensure the reappearance of the 298 K emission band at 540 nm.

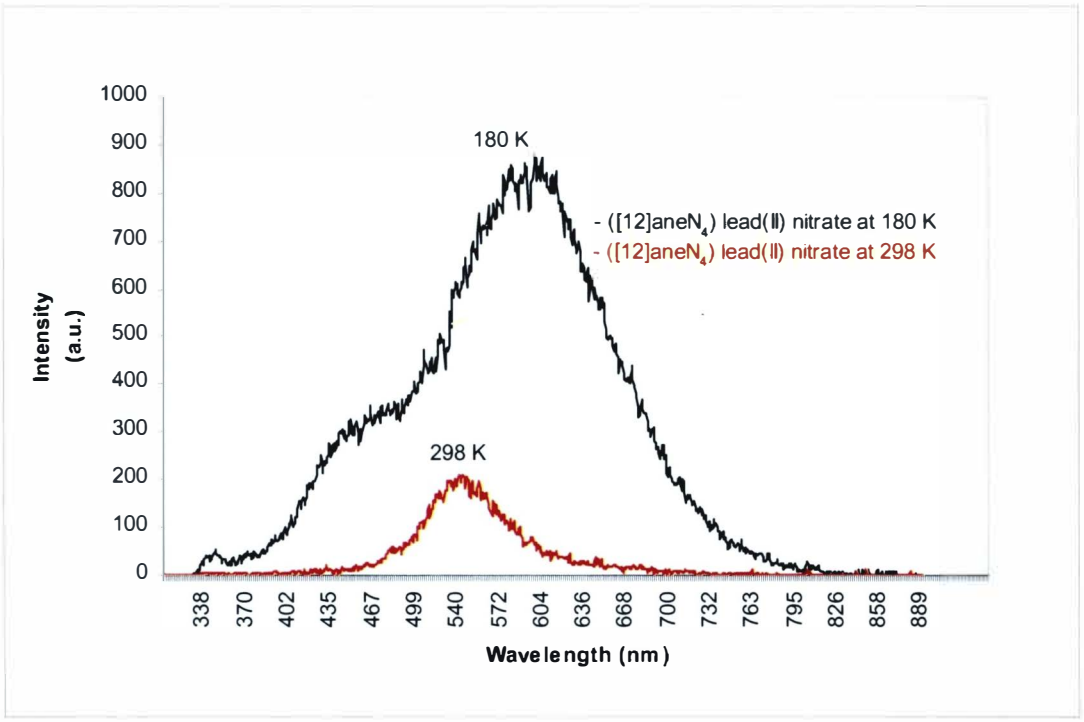

The luminescence spectrum in red was taken after warming the solution to 298 K. Both spectra were recorded with a 266 nm excitation, 180 ns delay, 5 μs gate width, and a 2 second exposure time.

Figure 15. Low Temperature Luminescence Spectrum of ([12]aneN$_4$) lead(II) nitrate in Propylene Carbonate at 180 K.

As can be seen in Figure 15, the emission maximum at 540 nm did not exist when the sample was cooled to 180 K. Instead a red shift occurred; thus, there was a new emission maximum located at 596 nm. A second emission component was detected at 460 nm. In addition to the presence of the two components at low temperature, the lifetimes of the low temperature components differed from the lifetime of the room temperature species (Table 2).

Table 2: Lifetimes for ([12]aneN$_4$) lead(II) nitrate at 298 K and 180 K.

Temperature (K)	τ_{460nm} (μs)	τ_{540nm} (μs)	τ_{596nm} (μs)
298	---	5.47 +/- 0.36	---
180	2.94 +2.97%	8.47 +4.84%	18.5 +2.16%

The +/- for tabulated values indicates that the standard deviation was calculated for the collected data. The + % for tabulated values indicates that the percent difference was calculated for the collected data.

Table 2 demonstrates the existence of two unique components for the complex in solution at 180 K because the lifetime for each species is clearly different. Thus, cooling of the sample to a glassy medium resulted in the complex having a temperature dependent emission spectrum.

At 298 K, the complex displays a 540 nm emission band that may be due to a small energy gap between two ^1G microstates of the d^2 ion under the influence of an octahedral field or a small gap between the $^3P_2$ and $^3P_1$ states of the *s-p* mixed s^2 ion. The observed lifetime for the complex at 298 K demonstrated that relaxation from the excited singlet or triplet state via phosphorescence occurs. Upon cooling to 180 K, the complex no longer exhibited the 540 nm emission band. The appearance of two components appeared with unique observed lifetimes for each band, the low temperature blue and red emission bands. The photophysical behavior of the complex may be due to an increase in separation between the microstates of the excited singlet or triplet state.

([14]aneN$_4$) lead(II) nitrate

Successful complexation of the free ligand, [14]aneN$_4$, with $Pb(NO_3)_2$ was

verified with the use of IR and NMR spectroscopy. In addition, X-ray information was obtained on the crystalline complex.

The IR spectrum for the free ligand displayed secondary N-H stretching at ~3200 cm^{-1} and asymmetric and symmetric C-H stretching at ~2900 cm^{-1} and ~2800 cm^{-1} respectively (Figure 16).

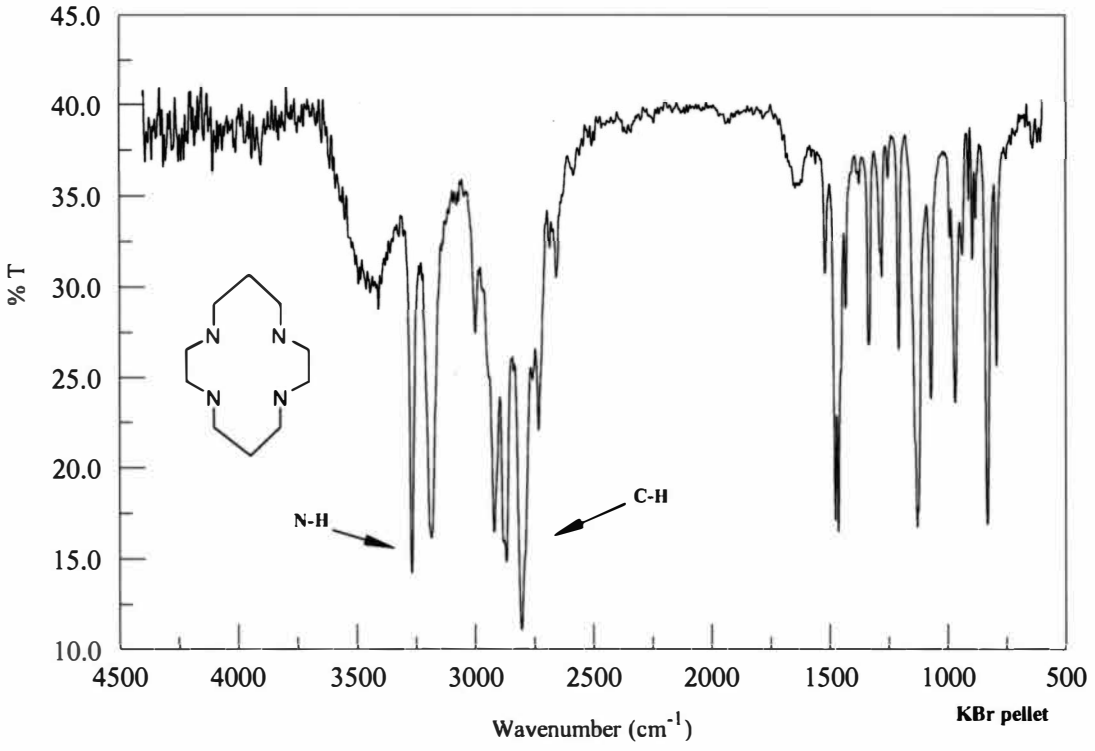

Hydrogens on the nitrogens are not shown.

Figure 16. The IR Spectrum of the Free Ligand, [14]aneN_4.

As seen with ([12]aneN_4) lead(II) nitrate, ([14]aneN_4) lead(II) nitrate showed shifts in the N-H and C-H stretching (3244 cm^{-1}, ~2990 cm^{-1}, and 2862 cm^{-1}, respectively) ; also, there was the presence of the shifted N-O stretch from the nitrate counterions present at ~1385 cm^{-1}. The IR spectrum is shown in Figure 17.

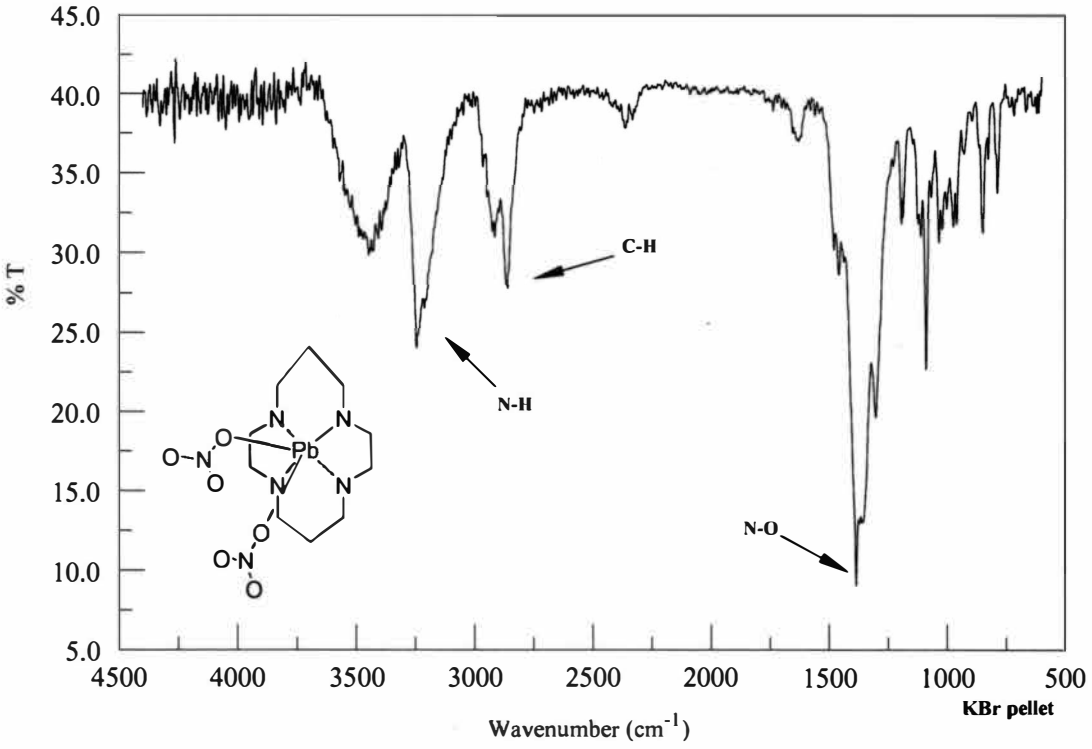

Hydrogens on the nitrogens are not shown.

Figure 17. The IR Spectrum of ([14]aneN$_4$) lead(II) nitrate.

A comparison between the ^{13}C NMR spectra for the free ligand and complex displayed a change in symmetry of the molecule upon complexation, unlike ([12]aneN$_4$) lead(II) nitrate. The free ligand had three different resonances; whereas, the complex had 5 different resonances. The next two figures show the ^{13}C NMR spectra for [14]aneN$_4$ and ([14]aneN$_4$) lead(II) nitrate.

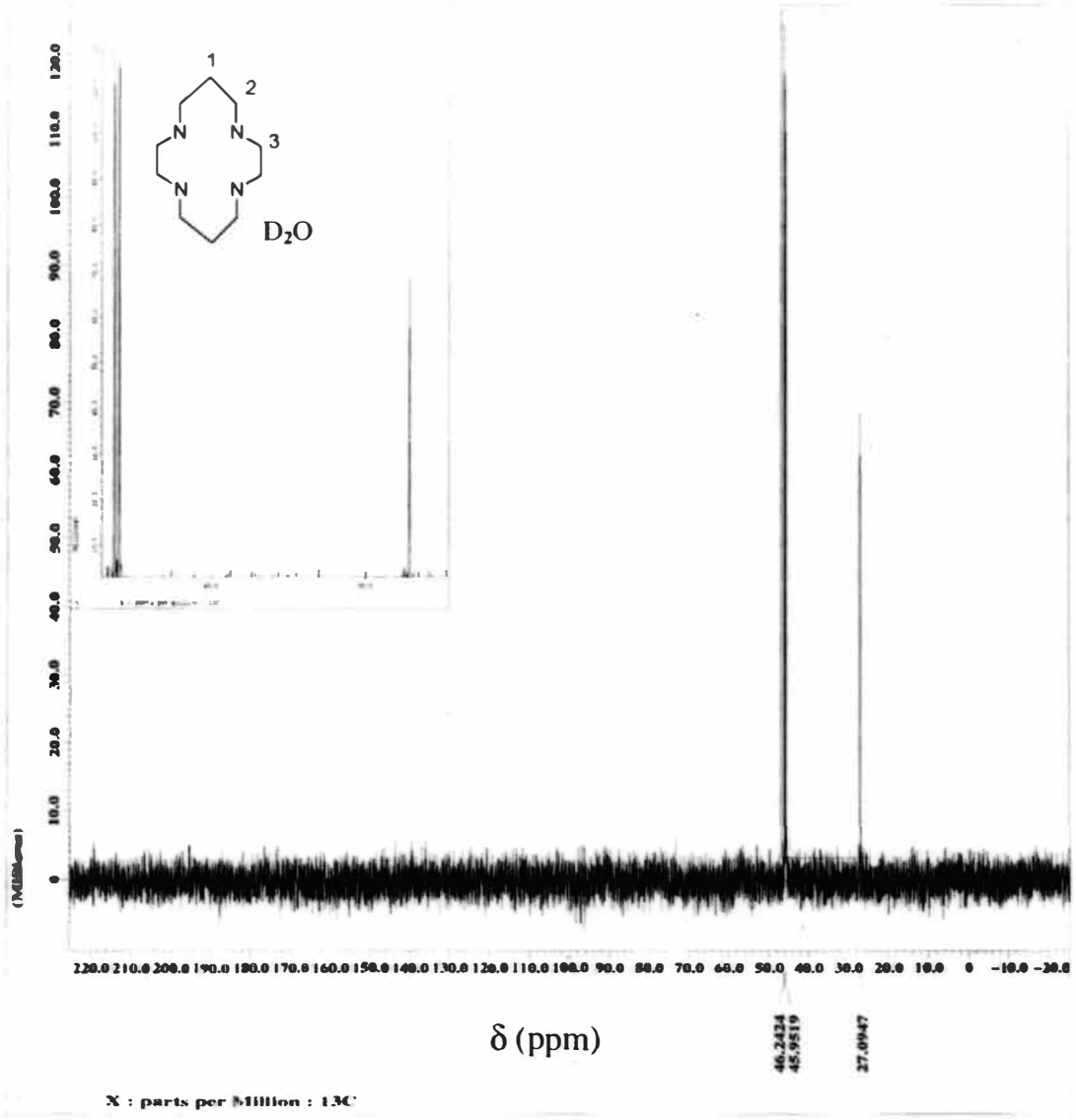

Figure 18. ^{13}C NMR Spectrum of [14]aneN_4 in D_2O at 298 K.

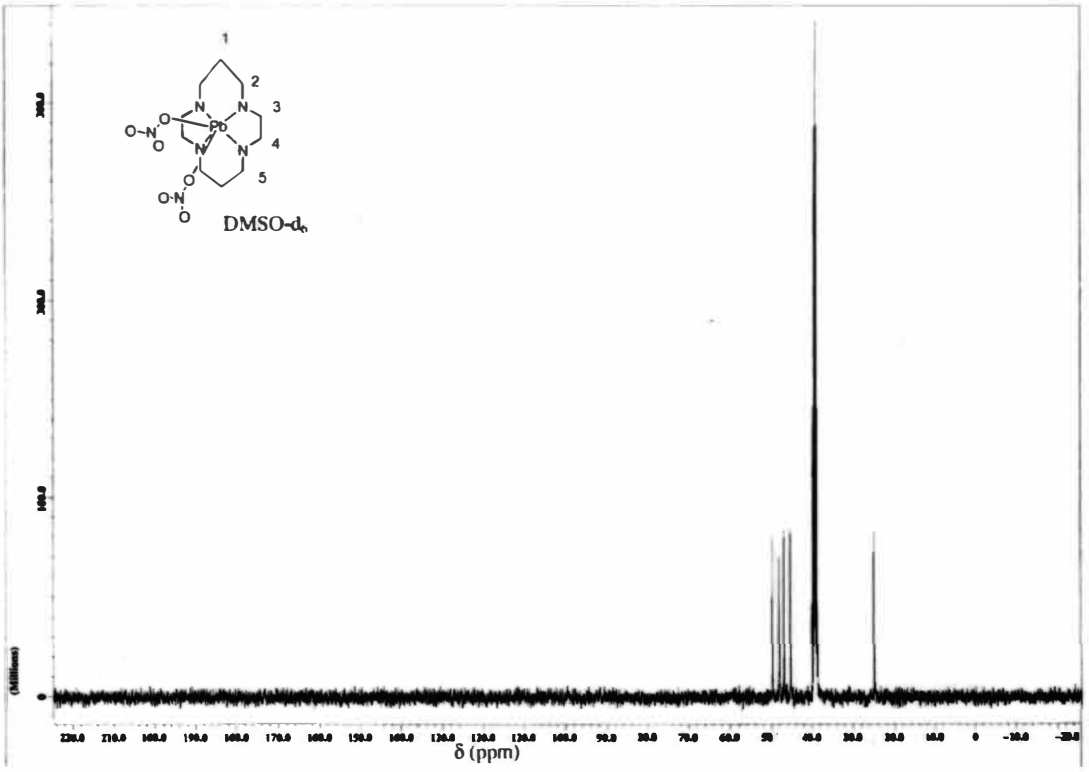

Figure 19. ^{13}C NMR Spectrum of ([14]aneN$_4$) lead(II) nitrate in DMSO-d$_6$ at 298 K.

Figure 19 shows a departure from the symmetry present in the free ligand (Figure 18); as a result, the complex was proven not to be the free ligand in solution.

An X-ray analysis was done on the crystalline complex. The x-ray quality crystals of the complex were monoclinic, and the space group was determined to be $P2_1/c$. The structure refined to an R-value of 8.07%. The bond lengths and angles of interest are listed in Table 3. The structural diagram labeled with the atoms of interest is shown in Figure 20.

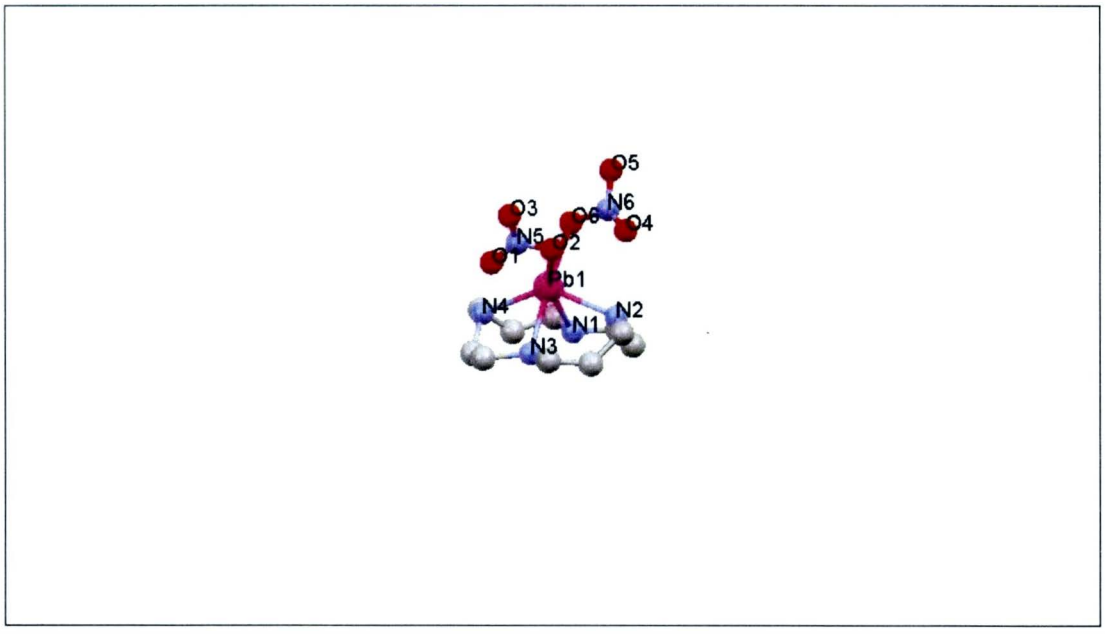

The color scheme is: C (gray), N (blue), O (red), Pb (pink). Atoms of interest are labeled.

Figure 20. Structure of ([14]aneN$_4$) lead(II) nitrate.

Table 3: Selected Bond Lengths (Å) and Angles (degrees).

Bond Lengths			
Pb(1) – N(1)	2.461	N(5) – O(1)	1.202
Pb(1) – N(2)	2.490	N(5) – O(2)	1.190
Pb(1) – N(3)	2.447	N(5) – O(3)	1.286
Pb(1) – N(4)	2.567	N(6) – O(4)	1.124
Pb(1) – O(2)	2.879	N(6) – O(5)	1.270
Pb(1) – O(6)	2.895	N(6) – O(6)	1.343

Table 3-Continued

Bond Angles			
Pb(1) – N(1) – N(4)	53.14	Pb(1) – N(3) – N(2)	52.06
Pb(1) – N(1) – N(2)	55.37	Pb(1) – N(3) – N(4)	56.43
Pb(1) – N(2) – N(1)	54.42	Pb(1) – N(4) – N(1)	50.06
Pb(1) – N(2) – N(3)	50.82	Pb(1) – N(4) – N(3)	52.57

Table 3 data was used in conjunction with computational software in order to calculate the distance that lead(II) rests above the plane of nitrogens in [14]aneN_4. Lead(II) rests 1.393 Å above the macrocycle, which is less than what was found for ([12]aneN_4) lead(II) nitrate. Thus, as the macrocyclic size is increased the distance lead(II) resides above the plane of the tetraaza framework is decreased.

This difference in geometry gives rise to a unique UV-Vis spectrum of the complex, which is clearly different from that of ([12]aneN_4) lead(II) nitrate (Figure12). The spectrum for ([14]aneN_4) lead(II) nitrate was compared to that of the free ligand, $Pb(NO_3)_2$, and the solvent. The comparison of the spectra confirmed the species observed was of the complex itself. The complex absorbed radiation in the ultraviolet region of the electromagnetic spectrum; in addition, the spectrum displayed in Figure 21 shows a maximum at 257 nm.

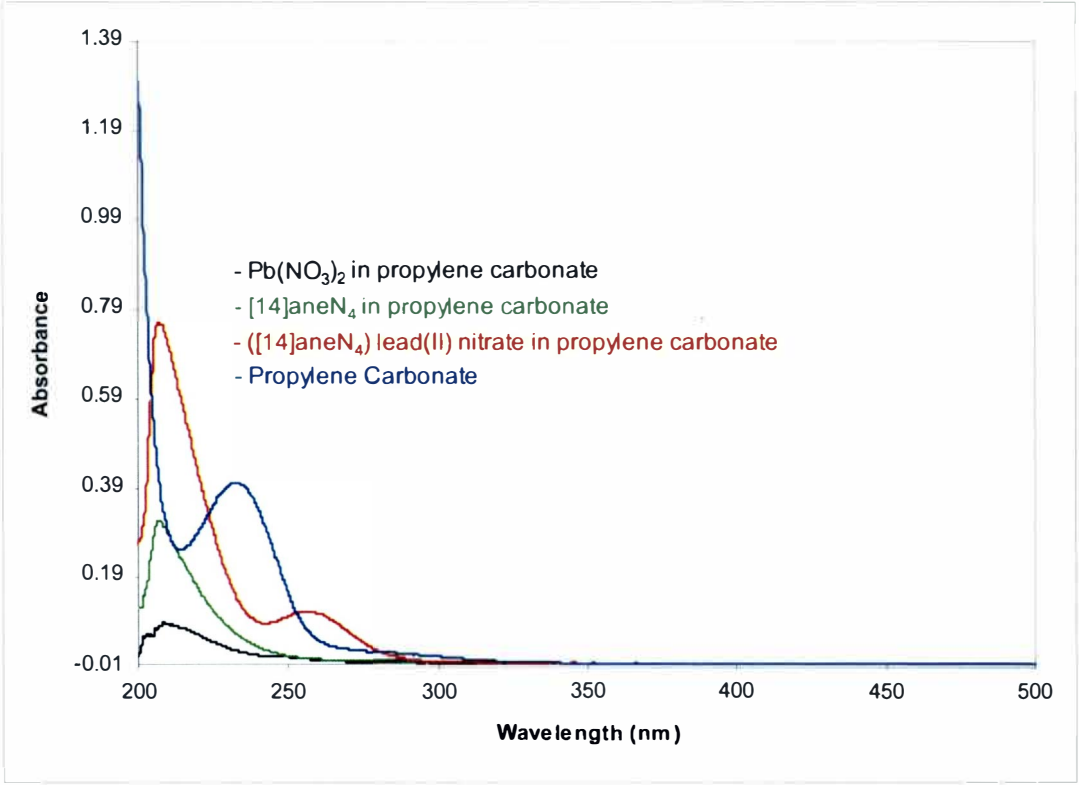

All solids were dissolved in propylene carbonate. All the UV-vis spectra for the solid samples dissolved in propylene carbonate were solvent subtracted.

Figure 21. UV-vis Spectra of ([14]aneN$_4$) lead(II) nitrate, [14]aneN$_4$, Pb(NO$_3$)$_2$, and Propylene Carbonate at 298 K.

The complex shown in Figure 21 had a molar absorbtivity of 1000 L mol^{-1} cm^{-1}. Excitation of the sample at 266 nm was possible, due to the maximum at 257 nm.

The sample was excited at 266 nm, and a red emission band was observed at room temperature. This emission band was lower in energy than that observed for ([12]aneN$_4$) lead(II) nitrate. The new excited species was compared to that of the free ligand and solvent.

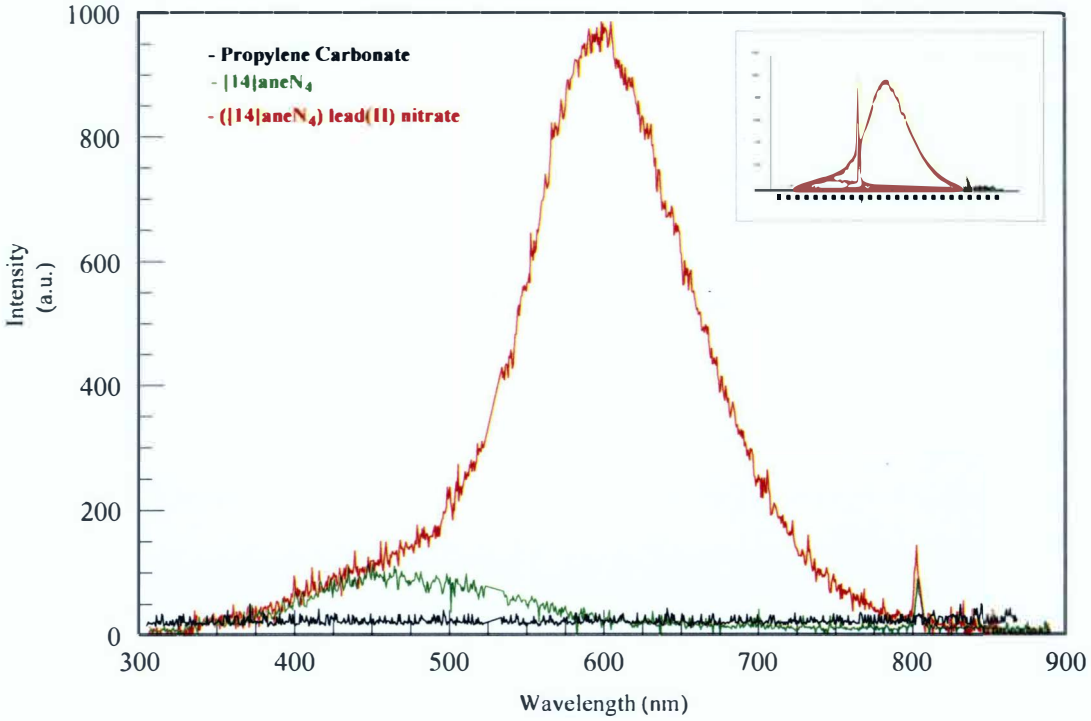

The complex is shown in red and is compared to the spectra for the free ligand (green) and the solvent (black). All samples were deaerated with He to avoid quenching by O_2; in addition, all variables for acquisition of the emitted light were kept the same (266 nm excitation; 180 ns delay; 5 μs gate width; 25 second exposure). A spike from charge build-up on the CCD was taken out of each spectrum and the data points were interpolated from 523.68 nm to 533.99 nm (inset shows spike). A laser spike is present near 800 nm.

Figure 22. Luminescence Spectrum of ([14]aneN$_4$) lead(II) nitrate in Propylene Carbonate at 298 K.

The complex's emission spectrum was unique from that of the solvent and free ligand with a maximum at 600 nm; in addition, the emission band differed in energy from that of ([12]aneN$_4$) lead(II) nitrate (Figure 13). A long lifetime exhibited by the ([14]aneN$_4$) lead(II) nitrate excited species was indicative of phosphorescence as well (18); the lifetime of the complex was 1.30 +/- 0.08 μs. The large molar absorbtivity of the complex suggested that a spin allowed transition occurred, which was found for the [12]aneN$_4$ complex as well. However, due to the presence of the

heavy atom, lead, intersystem crossing was facilitated. Thus, the emissive behavior detected was from a relaxed spin-forbidden transition. At low temperature, 180 K, the sample exhibited two components versus the single component found at room temperature. Regardless of the two components being different, this type of low temperature behavior was seen for the [12]aneN_4 complex as well.

The wavelength of the red emission band seen at 180 K for ([14]aneN_4) lead(II) nitrate had a different emission maximum than the red emission band seen at 298 K. The room temperature emission band had a red shift from 600 nm to 612 nm. The blue component had a maximum of 470 nm. Each low temperature band had a unique lifetime. After cooling, the sample was warmed to room temperature in order to ensure that the original 600 nm band returned at room temperature. Figure 23 displays the results from the low temperature analysis.

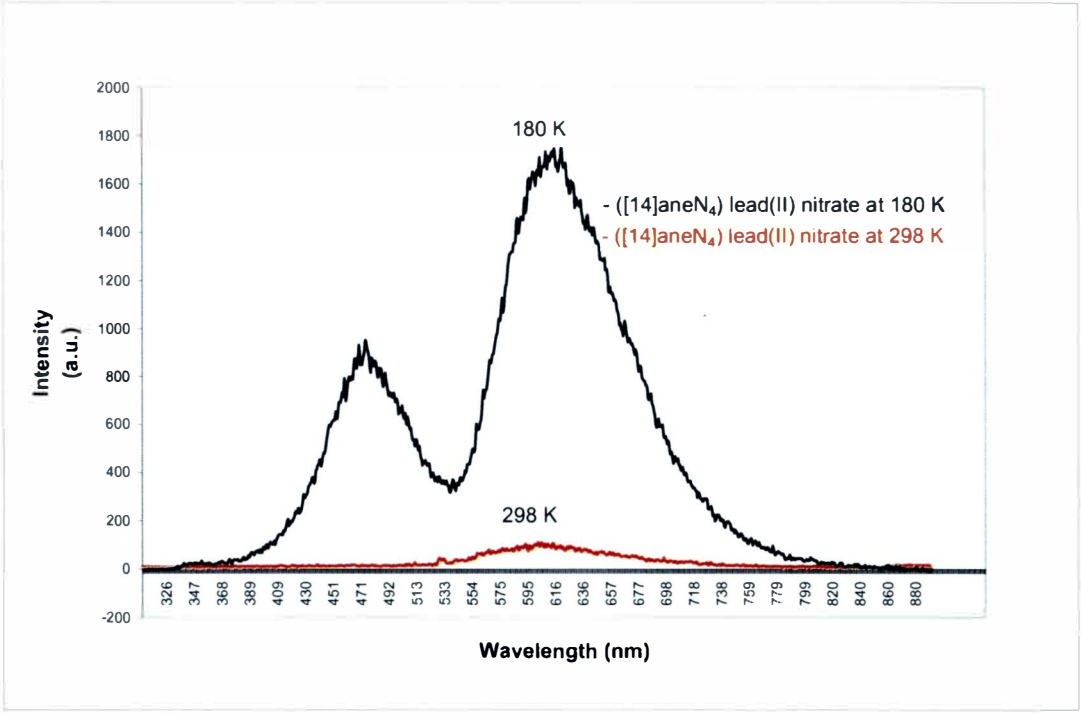

The luminescence spectrum in red was taken after warming the solution to 298 K. Both spectra were recorded with a 266 nm excitation, 180 ns delay, 5 μs gate width, and a 2 second exposure time.

Figure 23. Low Temperature Luminescence Spectrum of ([14]aneN$_4$) lead(II) nitrate in Propylene Carbonate at 180 K.

The emission response of the complex at low temperature suggests that as the energy gap between the two excited states becomes large a competition between the two excited states exists. At higher temperatures, this competition is not seen. In addition to the observed spectral differences, the lifetimes of the complex at 298 K and at 180 K were obtained. The lifetimes are shown in Table 4.

Table 4: Lifetimes for ([14]aneN$_4$) lead(II) nitrate at 298 K and 180 K.

Temperature (K)	τ_{470nm} (μs)	τ_{600nm} (μs)	τ_{612nm} (μs)
298	---	1.30 +/- 0.08	---
180	0.826 +14.1%	21.7 +2.25%	22.7 +2.58%

The +/- for tabulated values indicates that the standard deviation was calculated for the collected data. The + % for tabulated values indicates that the percent difference was calculated for the collected data.

While there is a clear increase in lifetime upon cooling of the sample by ~20 times that of room temperature, we can only propose the possibility that the energy gap between the two excited states (shown in Figure 1 and Figure 2) becomes large. However, this energy gap is not the same as that for ([12]aneN$_4$) lead(II) nitrate because of the significant differences in photophysical properties between the two complexes.

([15]aneN$_4$) lead(II) nitrate

The IR spectrum of the complex was compared to that of the free ligand and $Pb(NO_3)_2$, as was done with previous complexes. Also, elemental analysis was performed on the complex to verify the composition of the newly formed tetraaza complex. The percent yield of this new complex was low, a 1.9% yield. The IR spectrum of the free ligand, Figure 24, displays N-H stretching ~3271 cm^{-1}, asymmetric C-H stretching ~2913 cm^{-1}, and symmetric C-H stretching ~2809 cm^{-1}.

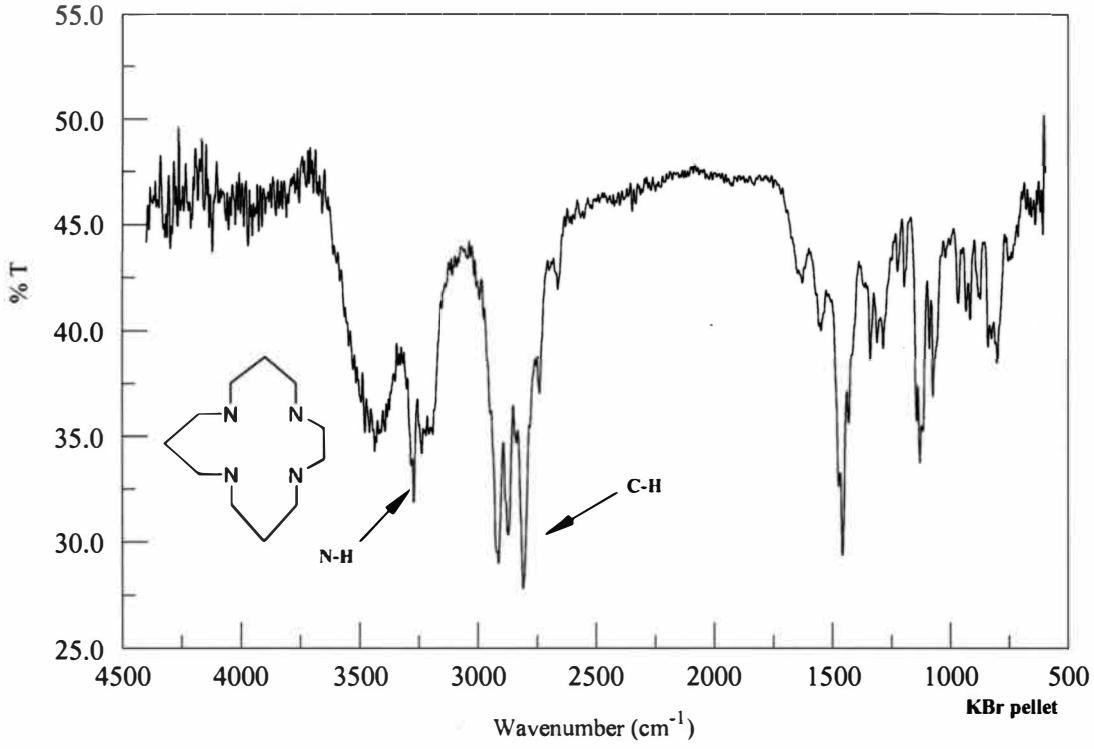

Hydrogens on the nitrogens are not shown.

Figure 24. The IR Spectrum of the Free Ligand, [15]aneN_4.

In contrast to the IR spectrum of the free ligand, the IR spectrum of the complex, Figure 25, displays shifted N-H and C-H stretching: N-H stretch at ~3206 cm^{-1}, C-H asymmetric stretch at ~2900 cm^{-1}, and symmetric C-H stretch at ~2852 cm^{-1}. A strong N-O stretch, characteristic of the nitrate group, was identified at ~1384 cm^{-1}. Similar shifting of these pertinent frequencies were seen with the previous complexes.

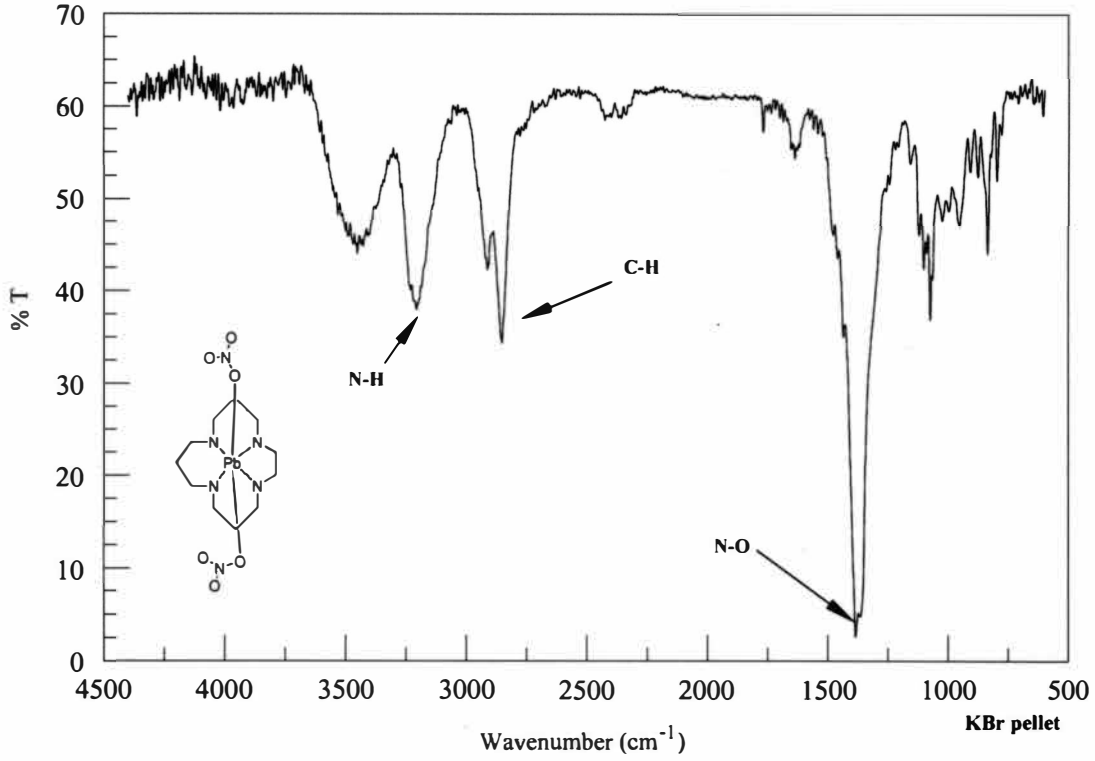

Hydrogens on the nitrogens are not shown.

Figure 25. The IR Spectrum of ([15]aneN$_4$) lead(II) nitrate.

The elemental analysis results suggested that a half of a water molecule was included in the coordination sphere of lead(II): %C 23.98, %H 5.07, %N 15.14. Based upon the calculated distances for lead(II) above the tetraaza plane for the previous complexes investigated, lead(II) extended ~1.353 Å above the tetraaza plane of [15]aneN$_4$.

In addition to the verification methods shown above, the UV-Vis spectrum of the complex was obtained. The samples (free ligand and complex) were dried and placed into propylene carbonate for analysis. The absorbance maxima for the solvent, $Pb(NO_3)_2$, [15]aneN$_4$, and ([15]aneN$_4$) lead(II) nitrate were all unique (Figure 26). Thus, the absorption band for the complex was due to the presence of the lead(II)

center within the tetraaza macrocyclic framework.

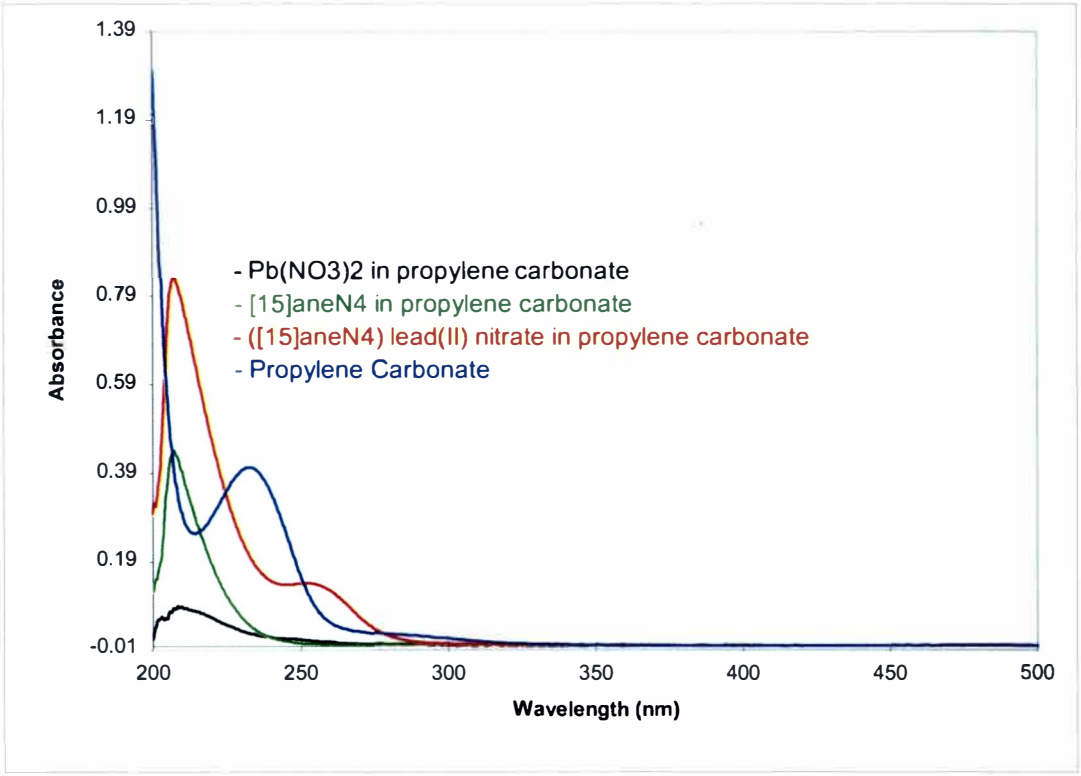

All solids were dissolved in propylene carbonate. All the UV-vis spectra for the solid samples dissolved in propylene carbonate were solvent subtracted.

Figure 26. UV-vis Spectra of ([15]aneN$_4$) lead(II) nitrate, [15]aneN$_4$, Pb(NO$_3$)$_2$, and Propylene Carbonate at 298 K.

The complex absorbed at 253 nm, which made excitation of the sample at 266 nm possible. In addition, the complex had a molar absorbtivity of 1200 Lmol^{-1}cm^{-1}. The large molar absorbtivity suggested that the complex underwent a spin-allowed transition upon absorption of radiation like the other two complexes.

However, ([15]aneN$_4$) lead(II) nitrate was weakly emissive, with a quantum yield of 0.00014, at room temperature. The emission band was located at ~588 nm. This 588 nm band had a lifetime of 0.626 +/- 0.030 μs at room temperature. As a

result, the long lifetime of the complex was due to radiative relaxation from a spin-forbidden excited state back down to the ground state (23). The emission band is shown in Figure 27, and was compared to that of the free ligand and solvent.

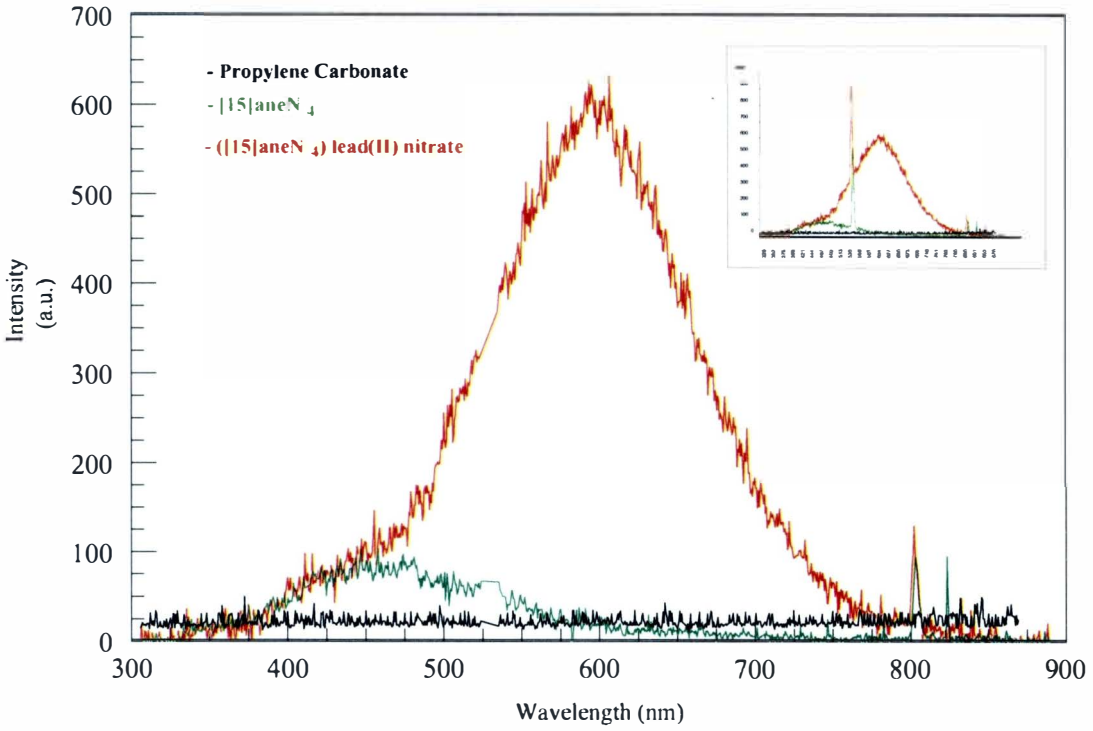

The complex is shown in red and is compared to the spectra for the free ligand (green) and the solvent (black). All samples were deaerated with He to avoid quenching by O_2; in addition, all variables for acquisition of the emitted light were kept the same (266 nm excitation; 180 ns delay; 5 μs gate width; 25 second exposure). A spike from charge build-up on the CCD was taken out of each spectrum and the data points were interpolated from 524.25 nm to 534.56 nm (inset shows spike). A laser spike is present near 800 nm.

Figure 27. Luminescence Spectrum of ([15]aneN$_4$) lead(II) nitrate in Propylene Carbonate at 298 K.

In addition to the observed emission band for the complex shown in the above figure, the emission band was sensitive to quenching by oxygen. Quenching by O_2 occurred for the [12]aneN$_4$ and [14]aneN$_4$ complexes as well. The low temperature

behavior of the complex was investigated; as a result, the complex displayed two emission bands at 180 K. The band at 612 nm was more intense than the blue component at 460 nm. The original 588 nm band was obtained upon warming the sample to 298 K. The low temperature bands are shown in Figure 28.

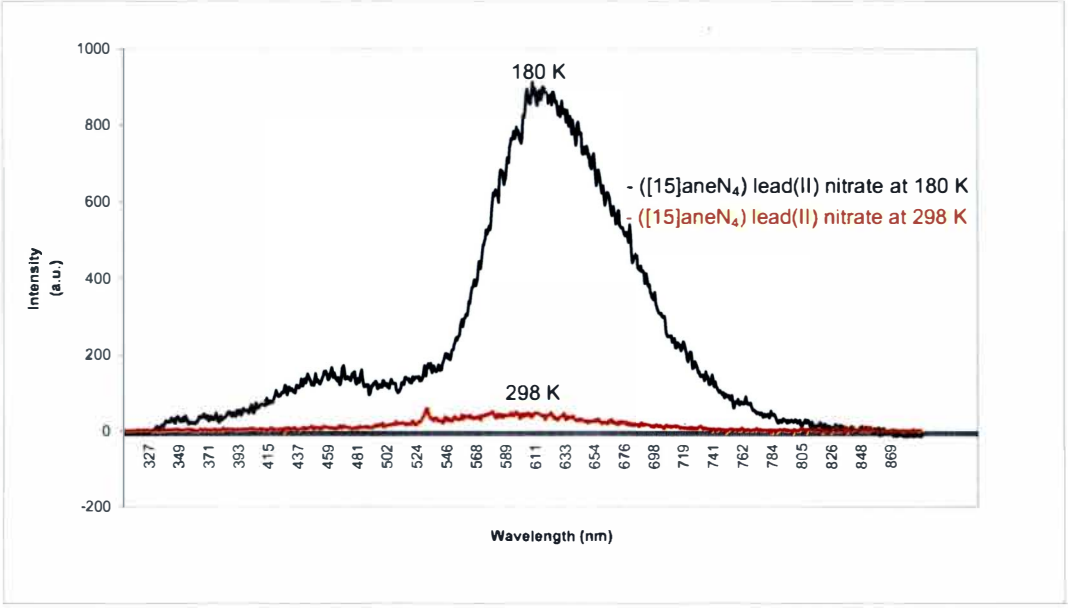

The luminescence spectrum in red was taken after warming the solution to 298 K. Both spectra were recorded with a 266 nm excitation, 180 ns delay, 5 μs gate width, and a 2 second exposure time.

Figure 28. Low Temperature Luminescence Spectrum of ([15]aneN$_4$) lead(II) nitrate in Propylene Carbonate at 180 K.

The low temperature spectrum suggests that competition between two excited states is occurring. As the temperature is lowered, the energy gap between the two states is increased. Thus, population of both states was detected at low temperature and not at room temperature. The radiative relaxation from the low temperature states had different lifetimes in support of the above observation. The lifetime comparison is shown in Table 5.

Table 5: Lifetimes for ([15]aneN$_4$) lead(II) nitrate at 298 K and 180 K.

Temperature (K)	τ_{460nm} (μs)	τ_{588nm} (μs)	τ_{612nm} (μs)
298	---	0.626 +/- 0.030	---
180	0.971 +0.920%	5.00 +4.94%	17.54 +2.23%

The +/- for tabulated values indicates that the standard deviation was calculated for the collected data. The + % for tabulated values indicates that the percent difference was calculated for the collected data.

Based upon differences in the lifetimes observed for the complex at room temperature and at low temperature we can propose that there are two observed populations and that these species are temperature dependent. Also, low temperature dependence was observed for the [12]aneN$_4$ and [14]aneN$_4$ complexes.

CHAPTER III

DISCUSSION ON THE TETRAAZA LEAD(II) COMPLEXES

A Comparison at 298 K

Relevance of an Ambient, 298 K, Comparison

The purpose of this investigation was to discover ways in which to express the sensing of lead(II) itself through manipulation of the Pb-tetraaza plane. If a lead(II) sensing kit was to be designed in the future, room temperature operating conditions become imperative. Low temperature emission responses would require the use of cryogenic conditions, which is not a sensible approach for field work. Thus, a comparison of the complexes under these conditions is relevant to future sensor design.

Geometry of the Complexes

The X-ray data obtained for ([12]aneN_4) lead(II) nitrate and ([14]ane) lead(II) nitrate displayed Pb-N bond lengths on the order of 2.461 Å to 2.569 Å, which was indicative of 'active' (hemidirected) complexes (3,18,20). As the macrocycle's size increased, the Pb-N bond lengths shortened; thus, it was possible to predict the nature of the Pb-N bonds for ([15]aneN_4) lead(II) nitrate. ([15]aneN_4) lead(II) nitrate should demonstrate shorter Pb-N bond lengths than the other two complexes, which correspond with the stereochemical activity of the inert s^2 lone pair of lead. Each complex in our family had a stereochemically active lead(II) center. Based on Belmer's previous investigation (21) on the relationship of the emissive nature of lead(II) and the optical response to the stereochemical activity of the lone s^2 pair, we

predicted that our complexes would be luminescent. Our 'active' complexes would result in the emission being turned on. However, the distance that lead(II) rests above the tetraaza framework will alter the emissive response of the complex in solution. Structural data obtained on each individual complex gave the following distances (Table 6):

Table 6: Distances for Pb^{2+} above the Tetraaza Framework.

Complex	Pb Distance above Tetraaza Plane (Å)
([12]aneN$_4$) lead(II) nitrate	1.472
([14]aneN$_4$) lead(II) nitrate	1.393
([15]aneN$_4$) lead(II) nitrate	1.353[1]

We proposed that the observed emission intensity would correspond to the distance; for example, ([12]aneN$_4$) lead(II) nitrate had the longest distance from the tetraaza plane and would be the most emissive in the series. While there is no known information on the exact nature of the excited states of complexes listed in Table 6, previous investigations on lead(II) halides have suggested that the excited state was due to an sp excited state of lead (13,17). Vogler and Nikol implemented that stereochemically active complexes tend to be distorted in the ground state and that the distortion is eliminated in the lowest excited state (17). We suggest that it may be possible for lead(II) to manifest *d-d* transitions rather than the *s-p* transitions examined by Vogler and Nikol. Regardless of the transitions being of s^2 or d^2 in

[1] The distance of lead(II) from the tetraaza plane of [15]aneN$_4$ was calculated using the difference in the tetraaza plane distances for ([12]aneN$_4$) lead(II) nitrate and ([14]aneN$_4$) lead(II) nitrate. This difference was divided by the amount of added carbons to the macrocyclic frame ((1.472 Å – 1.393 Å) /2 additional carbons = 0.040 Å / 1 additional carbon).

nature, our data serves to examine the dependency of the excited state on the initial ground state geometries of the tetraaza complexes.

Ambient UV-vis Spectra

Each complex absorbed in the ultraviolet region of the electromagnetic spectrum; also, each complex had a unique absorption maximum and shape. This was suggestive of each species being unique in solution. Propylene carbonate, a non-coordinating solvent, was used as the solvent system for each sample analyzed, Figure 29.

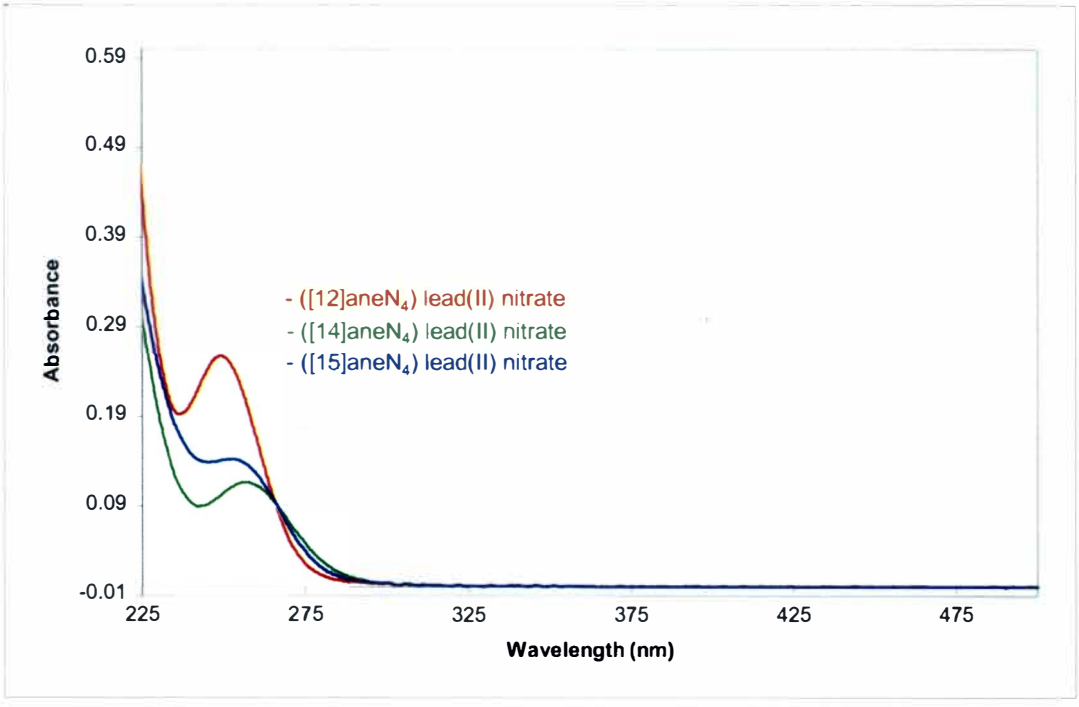

All solids were dissolved in propylene carbonate and were absorbance matched at 266 nm (A = 0.09).

Figure 29. UV-vis Spectra of ([12]aneN$_4$) lead(II) nitrate, ([14]aneN$_4$) lead(II) nitrate, and ([15]aneN$_4$) lead(II) nitrate in Propylene Carbonate at 298 K.

Figure 29 shows that the absorption spectrum for lead(II) is dependent on the size of the macrocycle. The individual analyses done on each complex demonstrated that the spectra shown in Figure 29 were not due to the ligand, $Pb(NO_3)_2$, or the solvent system. The unique species observed for each complex is due to a difference in geometry. The molar absorbtivity data calculated for each complex located in Table 7 is in agreement with each species being unique.

Table 7: Molar Absorbtivities for the Complexes under Investigation.

Complex	λ_{max} (nm)	ε ($Lmol^{-1}cm^{-1}$)
([12]aneN$_4$) lead(II) nitrate	249	3080
([14]aneN$_4$) lead(II) nitrate	257	1000
([15]aneN$_4$) lead(II) nitrate	253	1200

The molar absorbtivity values obtained indicated that each complex had a spin-allowed transition from the ground state, since the values were on the order of 10^3. However, the difference in the magnitude indicates that the same transition may not be occurring for each complex.

Ambient Luminescence Spectra

While each complex was excited to a spin-allowed state, the luminescence spectrum of each complex indicated that a definite trend existed between the coordination environment of lead(II) and the optical response of lead(II) in solution. As lead(II) resided further from the tetraaza plane of the macrocyle, the emission response grew in intensity (Figure 30). In order to ensure accuracy of the trend, the samples were absorbance matched at 266 nm (Figure 29) and the acquisition of an emission response from each complex was repeated three times.

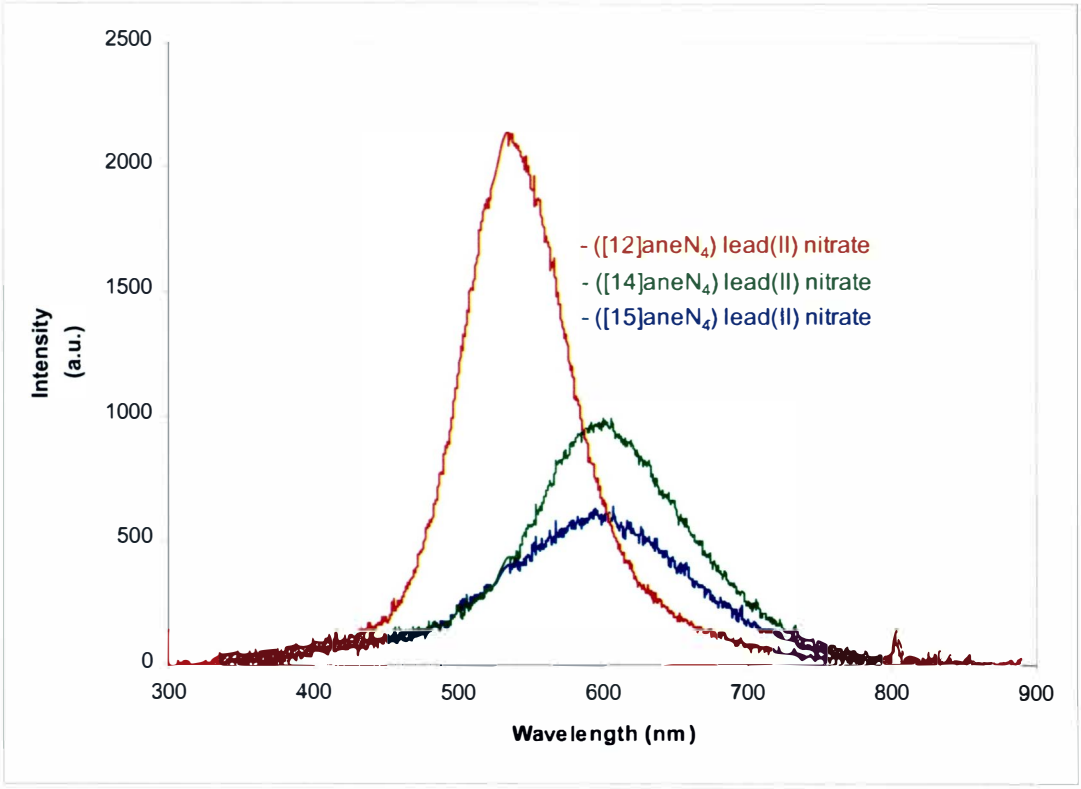

All samples were deaerated with He to avoid quenching by O_2; in addition, all variables for acquisition of the emitted light were kept the same (266 nm excitation; 180 ns delay; 5 μs gate width; 25 second exposure). A spike from charge build-up on the CCD was taken out of each spectrum and the data points were interpolated from 524.25 nm to 533.99 nm. A laser spike is present near 800 nm.

Figure 30. Luminescence Spectra of ([12]aneN$_4$) lead(II) nitrate, ([14]aneN$_4$) lead(II) nitrate, and ([15]aneN$_4$) lead(II) nitrate in Propylene Carbonate at 298 K.

According to Figure 30, there is a relationship between the lead(II) emission response and the lead(II) coordination environment under ambient conditions. While the analysis done on each individual complex suggested that the energy gap between two possible excited states was rather small, a comparison of each spectrum suggests the possibility that the energy gap may be affected by the geometry of the complex. As the distance lead(II) resides from the plane of the macrocycle increases, the energy

gap changes. ([12]aneN$_4$) lead(II) nitrate was approximately 2 times as intense as ([14]aneN$_4$) lead(II) nitrate and was approximately 3.5 times as intense as ([15]aneN$_4$) lead(II) nitrate. The ambient emission lifetimes and quantum yields obtained for the series are in agreement with the energy gap law; thus, the results in Table 8 suggest that non-radiative processes may become more important than radiative processes as the distance of lead(II) from the tetraaza plane decreases.

Table 8: Ambient Lifetimes and Quantum Yields for the Complexes under Investigation.

Complex	$\tau_{298K,\ He\ saturated}$ (μs)	$\phi_{298K,\ He\ saturated}$
([12]aneN$_4$) lead(II) nitrate	5.47 +/- 0.36	0.0011
([14]aneN$_4$) lead(II) nitrate	1.30 +/- 0.08	0.00020
([15]aneN$_4$) lead(II) nitrate	0.626 +/- 0.030	0.00014

While the exact nature of the excited state for each species in the series is not necessarily clear, ([12]aneN$_4$) lead(II) nitrate displayed a transition similar in energy to that found for lead(II) halides (13). ([14]aneN$_4$) lead(II) nitrate and ([15]aneN$_4$) lead(II) nitrate emitted at much lower energies than the lead(II) halides investigated by Vogler and Nikol. The lead(II) halide cluster investigated by Perkovic and Dutta did not display an intra-lead emission feature at room temperature (12).

The emission lifetimes of our complexes did demonstrate that intersystem crossing occurred; therefore, each complex underwent a spin-forbidden transition before relaxing back to the ground state via radiative decay. This radiative decay became weak as a consequence of the proximity of lead(II) to the tetraaza framework of the macrocycle. The distance between two possible excited states of lead(II) could be related to the Pb-tetraaza plane distance; such that, the energy gap increases with

increasing distance of lead(II) from the plane.

While further research on the emissive behavior of lead(II) in solution is necessary for a more quantitative analysis of the luminescence of lead(II) itself, our qualitative investigation suggests that an intricate relationship between coordination environment and the heavy atom analyte exists. The observed luminescence was due to lead(II) itself and depended on the stereochemical activity of the complex. By attaching lead(II) to a non-luminescent framework we were able to control the emission intensity of lead(II) itself by expanding the ring size of a tetraaza macrocycle. Radiative relaxation rates and quantum yields were dependent upon the change in geometry. As lead(II) is held further from the plane of the macrocycle, the emission band of lead(II) is shifted to higher energy, appears to become sharper, is longer lived, and is more emissive.

CHAPTER IV

FUTURE DIRECTIONS

Sulfur Donor Atoms

Future Interest

Future investigations of interest are to carry out further investigations on the tetraaza lead(II) nitrate family investigated in this study. The future experimentations are: solvent dependence experiments to obtain better quantum yields, concentration dependence experiments to obtain concentration values for detection, temperature dependent absorption studies, conformational analysis, the calculation of formation constants to obtain Pb/Zn selectivity data, and ^{207}Pb NMR spectroscopy.

Other investigations of interest are to increase the size of the macrocycle and to incorporate sulfur donor atoms into the ligand framework. While the nitrates were of interest in this investigation, their crystalline nature made the investigation limited in terms of solvent and excitation energy. Thiocyanates of the complexes investigated may provide a route to excitation at longer wavelengths.

The complex bis-(2, 2', 2"-triaminotriethylamine) lead(II) thiocyanate was synthesized in our laboratory, using Kokozay's and Sienkiewicz's complexation procedure for $Pb_3(en)_6(SCN)_6$ (24). Elemental analysis confirmed successful complexation of bis-(2, 2', 2"-triaminotriethylamine) lead(II) thiocyanate : %C 27.24, %H 5.90, %N 22.15.

The complex had an absorbance maximum at 304 nm in propylene carbonate; in addition, the complex continued absorbing radiation at 355nm. The observed absorption band allowed for excitation at 355 nm. Excitation at such a wavelength

diminishes the concern of solvent emission, which can be problematic at 266 nm.

Excitation of bis-(2, 2', 2"-triaminotriethylamine) lead(II) thiocyanate at 355 nm under ambient conditions resulted in an intense emission band located at 600 nm (Figure 31).

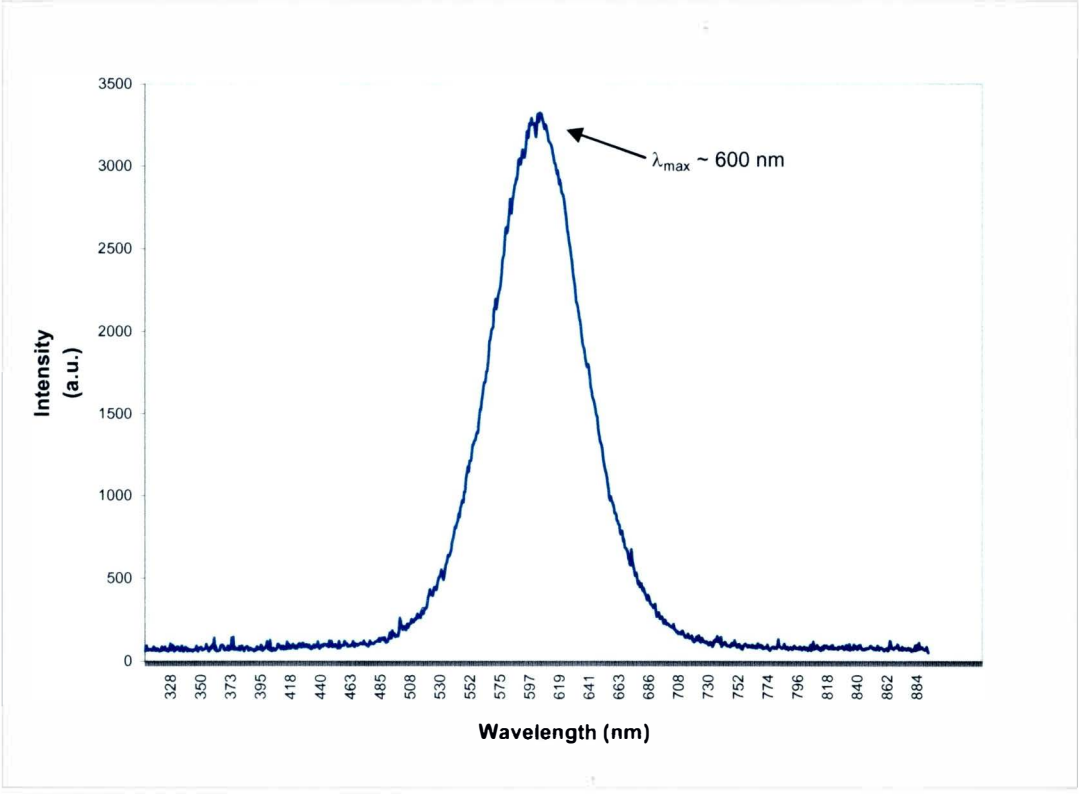

Excitation was at 355 nm with a 87 ns delay, 1000 ns gate width, and a 10 second exposure. The sample was deaerated with He to avoid quenching by O_2.

Figure 31. Luminescence Spectrum of Bis-(2, 2', 2"-triaminotriethylamine) lead(II) thiocyanate in Propylene Carbonate at 298 K.

Figure 31 suggests that the lead(II) thiocyanate complexes can be made to be highly luminescent at 298 K. Our result is promising for future lead(II) sensing design because it eliminates the problematic excitation wavelength, 266 nm.

Further research on lead(II) in solution is imperative for progress on sensing heavy metals. With a lead-containing environment in existence and with lead poisoning as a major health risk in today's growing society, the need for understanding the behavior of lead in solution becomes relevant. Little is known on the emissive nature of this heavy metal; however, previous investigations along with our investigation demonstrate that lead does emit itself (12,13,17), and the emission response can be controlled. Thus, the sensing abilities of the heavy metal analyte for itself should be of interest for decades to come.

CHAPTER V

METHODS

Protocol for the Analyte of Focus, Lead(II)

Synthesis of Ligands

[12]aneN$_4$ ((1, 4, 7, 10)-tetraazacyclododecane)

97% pure [12]aneN$_4$ was purchased from Sigma-Aldrich. ^{13}C NMR (DMSO-d_6): δ(ppm) 45.76.

[15]aneN$_4$ ((1, 4, 8, 12)-tetraazacyclopentadecane)

97% pure [15]aneN$_4$ was purchased from Sigma-Aldrich.

[14]aneN$_4$ ((1, 4, 8, 11)-tetraazacyclotetradecane

The ligand was synthesized using Barefield's (25) nickel(II) template synthesis with the starting material, 1, 5, 8, 12-tetraazadodecane, and 30% glyoxal. [14]aneN$_4$ was obtained after reduction of the nickel(II) complex with sodium tetrahydroborate. The ligand was recrystallized from chlorobenzene. (25) ^{13}C NMR (D_2O): δ(ppm) 46.24, 45.95, 27.09.

Synthesis of the Lead(II) Complexes

([14]aneN$_4$) lead(II) nitrate

A procedure analogous to that of Moore's procedure for ([14]aneN$_4$) lead(II)

nitrate was followed. 0.62 grams of $Pb(NO_3)_2$ was dissolved in 5 mL of dimethyl sulfoxide. Upon dissolution, 0.40 grams of [14]aneN_4 was added to the solution. The mixture was stirred for one hour, and the lead(II) complex was precipitated upon addition of methanol. The crystals were stored in the 'mother' liquor until further analysis was done. (26) IR (KBr): 3244 cm^{-1} (N-H), ~2990 cm^{-1} and 2862 cm^{-1} (C-H), 1385 cm^{-1} (N-O); ^{13}C NMR (DMSO-d_6): δ(ppm) 50.0, 48.9, 47.1, 45.5, 25.2.

([12]aneN_4) lead(II) nitrate and ([15]aneN_4) lead(II) nitrate

A modified version of Moore's procedure was used for ([12]aneN_4) lead(II) nitrate and ([15]aneN_4) lead(II) nitrate. $Pb(NO_3)_2$ was dissolved in 2.5 mL of dimethyl sulfoxide. The ligand was added to the solution, and the mixture was stirred for one hour. After mixing, the complex was precipitated by adding 2-4 mL of methanol and by vapor diffusion in an ether chamber. The chambers were placed into a freezer for further precipitation. After crystallization, the complexes were kept in the 'mother' liquor until further analysis was done. (26) ([12]aneN_4) lead(II) nitrate: IR (KBr): 3263 cm^{-1} (N-H), 2990 cm^{-1} and 2867 cm^{-1} (C-H), 1381 cm^{-1} (N-O); ^{13}C NMR (DMSO-d_6): δ(ppm) 45.8. ([15]aneN_4) lead(II) nitrate: IR (KBr): 3206 cm^{-1} (N-H), 2900 cm^{-1} and 2852 cm^{-1} (C-H), 1384 cm^{-1} (N-O); EA (([15]aneN_4) lead(II) nitrate • ½ H_2O): %C 23.98, %H 5.07, %N 15.14.

IR and ^{13}C NMR Spectroscopy

All infrared spectra were obtained with a Perkin Elmer 1710 FTIR spectrometer; in addition, all samples were prepared via KBr pellets. ^{13}C NMR spectra were recorded with a JEOL JNM-ECP400, with the samples prepared in DMSO-d_6 or D_2O.

Elemental Analysis

The certificates of analysis on ([15]aneN$_4$) lead(II) nitrate and Bis-(2, 2', 2"-triaminotriethylamine) lead(II) thiocyanate were obtained from Desert Analytics, Tucson, Arizona.

X-ray Determination of Lead(II) Complexes

Crystal data was obtained with Nonius Cad 4 X-ray diffraction equipment. Cif files were analyzed using Mercury 1.4.1.

UV-Vis Spectra and Molar Absorbtivities

All samples were recorded with a Shimadzu UV-2101 PC UV-Vis scanning spectrometer. Samples of the lead(II) complexes were dissolved in propylene carbonate and were absorbance matched to A = 0.09 at λ = 266 nm before luminescence analysis. The free ligands and $Pb(NO_3)_2$ were dissolved in propylene carbonate; also, the absorbance of the solvent itself was measured at 266 nm.

Molar absorbtivities, ε, were calculated by creating stock solutions of the lead(II) complexes in propylene carbonate. The absorbance value for the maximum wavelength was recorded in a 1 cm cell and used with the known solution concentrations to calculate the ε values.

Luminescence Spectra

Excitation of the samples in propylene carbonate was done with the 266 nm harmonic from a Continuum Surelite-I Nd:YAG laser (1.05 V, Q-SW delay at 183 μs). The energy output of the laser was consistent at 9.2 to 9.7 mJ. Emitted light was collected by a fiber optic with a 362 nm cut-off filter, and the luminescence spectra

were recorded using a Princeton Instruments CCD interfaced to an Acton 1/3m spectrograph. Samples were deaerated with He and compared to aerated samples. In addition, recorded spectra were compared to spectra obtained with the use of a negative focal length lens in order to confirm that the emission was a single photonic process. Sample temperatures were maintained using an Oxford Optistat liquid nitrogen cryostat. Device control and data manipulations were done with WinSpec32 2.5.

Room Temperature Luminescence Spectra

All spectra were recorded by inspecting an aerated or de-aerated sample for 25 seconds with a 180 ns delay and a 5 μs gate width. The next sample was tested immediately after the first; such that, the process was repeated at least three times to test repeatability of data. Each spectrum was analyzed and the spectra were averaged to obtain the room temperature luminescence spectrum.

Low Temperature Luminescence Spectra

Each sample was cooled to 220 K and to 180 K. After cooling and recording the signal for 2 seconds with a 180 ns delay and 5 μs gate width, the sample was warmed to room temperature and the emitted light was collected. All variables were kept constant for all three temperatures.

Photophysical Measurements

Quantum yield determinations were performed using He-purged, absorbance matched samples (A = 0.09 at λ = 266 nm) in propylene carbonate. The integrated intensity of the ([12]aneN_4) lead(II) nitrate sample was compared to the absorbance matched standard, $Ru(bpy)_3^{2+}$ ($\phi_{\text{propylene carbonate at 298K}}$ = 0.071 (27)). Quantum yields for

([14]aneN$_4$) lead(II) nitrate and ([15]aneN$_4$) lead(II) nitrate were determined by comparison to ([12]aneN$_4$) lead(II) nitrate, using the integrated intensities of the absorbance matched samples. (28) Luminescent lifetimes were determined by excitation of the samples with the 266 nm harmonic from a Continuum Surelite-I Nd:YAG laser (1.05 V, Q-SW delay at 183 μs). The emitted light was collected by a fiber optic interfaced to an Acton SP300i monochromator/Hamamatsu R928 PMT. The photomultiplier was held constant at –1100 V. Sixty-four averages were recorded and the data was fit, using a computer program developed in-house.

Distance of Lead(II) from the Tetraaza Plane for Each Complex

X-ray structural information was analyzed with the program Mercury 1.4.1. A plane was defined with the tetraaza framework for each macrocycle. The distance of lead(II) above the tetraaza plane was computed with the software.

BIBLIOGRAPHY

(1) Spiro, T. G.; Stigliani, W. M. *Chemistry of the Environment*; Prentice Hall: Upper Saddle River, NJ, 1996; pp 322-328.

(2) Kessel, I.; O'Connor, J. T. *Getting the Lead Out: The Complete Resource on How to Prevent and Cope with Lead Poisoning*; Plenum Trade: NY, 1997; pp 1-23.

(3) Claudio, E. S.; Godwin, H. A.; Magyar, J. S. Fundamental Coordination Chemistry, Environmental Chemistry, and Biochemistry of Lead(II). In *Progress in Inorganic Chemistry*, Vol. 51; Karlin, K. D., Ed.; John Wiley & Sons, Inc.: NY, 2003; pp 1-144.

(4) Claudio, E. S.; ter Horst, M. A.; Forde, C. E.; Stern, C. L.; Zart, M. K.; Godwin, H. A. 207Pb-1H Two Dimensional NMR Spectroscopy: A Useful New Tool for Probing Lead(II) Coordination Chemistry. *Inorg. Chem.* **2000,** *39*, 1391-1397.

(5) Chen, C.; Huang, W. A Highly Selective Chemosensor for Lead Ions. *J. Am. Chem. Soc.* **2002,** *124*, 6246-6247.

(6) Deo, S.; Godwin, H. A. A Selective, Ratiometric Fluorescent Sensor for Pb^{2+}. *J. Am. Chem. Soc.* **2000,** *122*, 174-175.

(7) Bissell, R. A.; de Silva, P.; Gunaratne, P. L.; Lynch, M.; Maguire, G. E. M.; Sandanayake, K. R. A. S. Molecular Fluorescent Signaling with 'Fluor-Spacer-Receptor' Systems: Approaches to Sensing and Switching Devices via Supramolecular Photophysics. *Chem. Soc. Rev.* **1992,** *21*, 187-195.

(8) Valeur, B.; Leray, I. Design principles of fluorescent molecular sensors for cation recognition. *Coord. Chem. Rev.* **2000,** *205*, 3-40.

(9) de Silva, A. P.; Gunaratne, H. Q. M.; Gunnlaugsson, T.; Huxley, A. J. M.; McCoy, C. P.; Rademacher, J. T.; Rice, T. E. Signaling Recognition Events with Fluorescent Sensors and Switches. *Chem. Rev.* **1997,** *97*, 1515-1566.

(10) Perkovic, M. W. Allosteric Manipulation of Photoexcited State Relaxation in $(bpy)_2Ru^{II}$(binicotinic acid). *Inorg. Chem.* **2000,** *39*, 4962-4968.

(11) Strasser, A.; Vogler, A. Intraligand phosphorescence of lead(II) β-diketonates under ambient conditions. *J. of Photochemistry and Photobiology A: Chem.* **2004,** *165*, 115-118.

(12) Dutta, S. K.; Perkovic, M. W. Lead as Its Own Luminescent Sensor. *Inorg. Chem.* **2002,** *41*, 6938-6940.

(13) Nikol, H.; Becht, A.; Vogler, A. Photoluminescence of Germanium(II), Tin(II), and Lead(II) Chloride Complexes in Solution. *Inorg. Chem.* **1992,** *31*, 3277-3279.

(14) Atkins, P.; de Paula, J. *Atkin's Physical Chemistry 7th Edition*; Oxford University Press: NY, 2001; pp 538-553.

(15) Lever, A. B. P. *Inorganic Electronic Spectroscopy*; Elsevier Publishing Company: NY, 1968; pp 1-18, 123-150.

(16) Kettle, S. F. A. *Physical Inorganic Chemistry: A Coordination Chemistry Approach*; Oxford University Press: NY, 1998; pp 156-182, 455-458.

(17) Vogler, A.; Nikol, H. The Structures of s^2 Metal Complexes in the Ground and sp Excited States. *Comments Inorg. Chem.* **1993,** *14*, 245-261.

(18) Hancock, R. D.; Shaikjee, M. S.; Dobson, S. M.; Boeyens, J. C. A. The Stereochemical Activity or Non-activity of the 'Inert' Pair of Electrons on Lead(II) in Relation to its Complex Stability and Structural Properties. Some Considerations in Ligand Design. *Inorganica Chimica Acta* **1988,** *154*, 229-238.

(19) Thom, V. J.; Hosken, G. D.; Hancock, R. D. Anomalous Metal Ion Size Selectivity of Tetraaza Macrocycles. *Inorg. Chem.* **1985,** *24*, 3378-3381.

(20) Shimoni-Livny L.; Glusker, J. P.; Bock, C. W. Lone Pair Functionality in Divalent Lead Compounds. *Inorg. Chem.* **1998,** *37*, 1853-1867.

(21) Belmer, N.; Perkovic, M. W. Personal Communication, 2006.

(22) Heeg, M. J. Personal Communication, 2006.

(23) Schulman, S. G. *Fluorescence and Phosphorescence Spectroscopy: Physicochemical Principles and Practice*; Pergamon Press: NY, 1977; pp 31-39.

(24) Kokozay, V. N.; Sienkiewicz A. V. Direct Synthesis and Crystal Structure of Lead(II) Thiocyanate Complex with Ethylenediamine. *Polyhedron* **1994,** *13*, 1427-1430.

(25) Barefield, E. K.; Wagner, F.; Herlinger, A. W.; Dahl, A. R. (1, 4, 8, 11-tetraazacyclotetradecane)Nickel(II) Perchlorate and 1, 4, 8, 11-tetraazacyclotetradecane. In *Inorganic Syntheses*, Vol. XVI; Basolo, F., Ed.; Mc-Graw Hill Book Co.: NY, 1976; pp 220-225.

(26) Alcock, N. W.; Herron, N.; Moore, P. Structural and Dynamic Behavior of Complexes of Lead(II) with Two Tetra-aza Macrocyclic Ligands as studied by X-Ray Crystallography and Natural-abundance Carbon-13 and Nitrogen-15 Nuclear Magnetic Resonance Spectroscopy. *J. C. S. Dalton* **1979,** 1486-1491.

(27) Caspar, J. V.; Meyer, T. J. Photochemistry of $Ru(bpy)_3^{2+}$. Solvent Effects. *J. Am. Chem. Soc.* **1983,** *105*, 5583-5590.

(28) Dupray, L. M.; Meyer, T. J. Synthesis and Characterization of Amide-Derivatized, Polypyridyl-Based Metallopolymers. *Inorg. Chem.* **1996,** *35*, 6299-6307.